



Royal Netherlands Institute for Sea Research

This is a pre-copyedited, author-produced version of an article accepted for publication, following peer review.

**Stratmann, T.; van Breugel, P.; Sweetman, A.K.; Van Oevelen, D.** (2023). Deconvolving feeding niches and strategies of abyssal holothurians from their stable isotope, amino acid, and fatty acid composition. *Mar. Biodiv.* 53(6). <https://dx.doi.org/10.1007/s12526-023-01389-2>

Published version: <https://dx.doi.org/10.1007/s12526-023-01389-2>

NIOZ Repository: <http://imis.nioz.nl/imis.php?module=ref&refid=381203>

[Article begins on next page]

The NIOZ Repository gives free access to the digital collection of the work of the Royal Netherlands Institute for Sea Research. This archive is managed according to the principles of the [Open Access Movement](#), and the [Open Archive Initiative](#). Each publication should be cited to its original source - please use the reference as presented.

1 **Deconvolving feeding niches and strategies of abyssal holothurians from their stable**  
2 **isotope, amino acid, and fatty acid composition**

3  
4 Tanja Stratmann<sup>1,2\*</sup>, Peter van Breugel<sup>3</sup>, Andrew K. Sweetman<sup>4</sup>, Dick van Oevelen<sup>3</sup>

5 <sup>1</sup>NIOZ Royal Netherlands Institute for Sea Research, Department of Ocean Systems (OCS), 't  
6 Horntje (Texel), The Netherlands.

7 <sup>2</sup>Utrecht University, Department of Earth Sciences, Utrecht, The Netherlands.

8 <sup>3</sup>NIOZ Royal Netherlands Institute for Sea Research, Department of Estuarine and Delta  
9 Systems (EDS), Yerseke, The Netherlands.

10 <sup>4</sup>Benthic Ecology and Biogeochemistry Research Group, The Scottish Association of Marine  
11 Science (SAMS), Scottish Marine Institute, Oban, UK.

12 \*Corresponding author: Tanja Stratmann, tanja.stratmann@nioz.nl

13  
14 **ORCID:**

15 Tanja Stratmann: 0000-0001-7997-1157

16 Andrew K. Sweetman: 0000-0002-9547-9493

17 Dick van Oevelen: 0000-0002-1740-5317

18  
19 **Abstract**

20 Holothurians are the dominant megabenthic deposit feeders in the Peru Basin (SE Pacific) and  
21 feed to various degrees of selectivity on a heterogenous pool of sedimentary detritus, but drivers  
22 of feeding selectivity and diet preferences for most holothurian species are unknown. This study  
23 reconstructs the diets of 13 holothurian species of the orders Elasipodida, Holothuriida, and  
24 Synallactida. Bulk stable isotope analyses ( $\delta^{13}\text{C}$ ,  $\delta^{15}\text{N}$ ) of holothurian body wall and gut wall  
25 tissues, gut contents, and feces were combined with compound-specific stable isotope analyses  
26 of amino acids, phospholipid-derived fatty acids, and neutral-lipid-derived fatty acids in the body  
27 wall. We further assessed how holothurians in the Peru Basin partition their resources and  
28 calculated how much of the daily particulate organic carbon (POC) flux to the area is ingested by  
29 them using information about gut contents of nine species. To assess the dependence of  
30 holothurians on fresh phytodetritus, we performed *in-situ* pulse-chase experiments using  $^{13}\text{C}$ - and  
31  $^{15}\text{N}$ -enriched phytodetritus. By measuring the uptake of this phytodetritus in fatty acids and  
32 amino acids, and by comparing it with the presence of these compounds in the sediment, we  
33 calculated net accumulation and net deficiency for specific fatty acids and amino acids, and  
34 discussed how climate change might affect the dependence on specific compounds.

35 A Sørensen–Dice coefficient-based cluster analysis using data from trophic levels, levels of  
36 heterotrophic re-synthesis of amino acids, feeding selectivity, and food sources/ diet suggested  
37 two major trophic groups with two optional subgroups each. Species-specific traits of  
38 locomotion, tentacle morphology, and gut structure likely allow resource partitioning and  
39 differences in selectivity among the holothurians, of which a subpopulation of 65% of all  
40 specimens can ingest 4 to 27% of the daily POC flux to the Peru Basin. Holothurians are  
41 specifically dependent on the uptake of arachidonic acid from phytodetritus, while most essential  
42 amino acids are available in the Peru Basin in sufficient concentrations.

43  
44 **Keywords:** Echinodermata, NLFA, PLFA, sea cucumber, diet, deep sea, biosynthetic pathway

45  
46 **Statements and Declarations:**

47 **Funding:** The research leading to these results has received funding from the European Union  
48 Seventh Framework Program (FP7/2007-2013) under the MIDAS project, grant agreement nr  
49 603418 and by the JPI Oceans – Ecological Aspects of Deep Sea Mining project under NWO-  
50 ALW grant 856.14.002 and BMBF grant 03F0707A-G. TS was further supported by the Dutch  
51 Research Council NWO (NWO-Rubicon grant no. 019.182EN.012, NWO-Talent program Veni  
52 grant no. VI.Veni.212.211).

53 **Conflict of Interest:** The authors declare that they have no conflict of interest.

54

55 **Ethical approval:** All applicable international, national, and/or institutional guidelines for  
56 animal testing, animal care and use of animals were followed by the authors.

57

58 **Sampling and field studies:** All necessary permits for sampling and observational field studies  
59 have been obtained by the authors from the competent authorities and are mentioned in the  
60 acknowledgements, if applicable. The study is compliant with CBD and Nagoya protocols.

61

62 **Data availability:** The datasets generated during and/or analyzed during the current study are  
63 available in the PANGAEA repository, **XXX**.

64

65 **Author Contribution Statement:** TS, DvO conceived the study; TS, DvO, AKS performed  
66 fieldwork; TS, PvB performed lab analysis; TS drafted the manuscript; TS, DvO, PvB, AKS  
67 contributed to revising the manuscript to its final version which was approved by all.

## 68 Introduction

69 Holothurians are abundant epifauna in the deep sea (Billett et al. 2001; Ruhl 2007; Alt et al.  
70 2013; Stratmann et al. 2018b) and they can be suspension or deposit feeders (Massin 1982). On  
71 soft sediment, deposit-feeding holothurians either dig into the sediment as funnel-feeders or  
72 conveyor belt-feeders or scavenge the surface sediment as rake feeders (Massin 1982). In this  
73 way, they take up particulate organic matter that is deposited on or buried in the sediment  
74 (Roberts et al. 2000), and some species have been shown to feed selectively for specific organic  
75 compounds (Ginger et al. 2001; Witbaard et al. 2001; Wigham et al. 2003a; Hudson et al. 2003):  
76 For example, the analysis of gut contents from holothurians collected at the Porcupine Abyssal  
77 Plain (PAP, NE Atlantic) showed that *Amperima rosea* Perrier, 1886, *Peniagone diaphana*  
78 Théel, 1882, and *Oneirophanta mutabilis mutabilis* Théel, 1879, feed selectively on fresh  
79 phytodetritus (Ginger et al. 2001; Witbaard et al. 2001; FitzGeorge-Balfour et al. 2010).  
80 However, when fresh phytodetritus is scarce, *O. mutabilis mutabilis* feeds on more refractory  
81 detritus material (FitzGeorge-Balfour et al. 2010) which is primarily consumed by the microbial  
82 community in its gut (Romero-Romero et al. 2021). Other species have a less selective feeding  
83 behavior, e.g., *Psychropotes longicauda* Théel, 1882, *Molpadiodemas villosus* Théel, 1886, and  
84 *Molpadia blakei* Théel, 1886, (FitzGeorge-Balfour et al. 2010). Though these examples suggest  
85 that that feeding selectivity and diet preferences of deep-sea holothurians are well known, the  
86 information is very rudimentary for most abyssal holothurian species (Billett 1991; Roberts et al.  
87 2000).

88  
89 Feeding selectivity of holothurians also affects the food availability for other benthic fauna. In  
90 fact, a non-linear regression analysis of individual biomass vs. biomass-specific phytodetritus  
91 carbon incorporation for nematodes, macrofauna and holothurians was highly significant  
92 (Stratmann et al. 2018a). This implies that larger organisms in the deep sea might be more  
93 important for or more efficient in exploiting labile phytodetritus than smaller organisms  
94 (Stratmann et al. 2018a). For example, in the Nazaré canyon (NE Atlantic), the whole population  
95 of *Molpadia musculus* Risso, 1826, removed approximately  $0.43 \pm 0.13$  g biopolymeric carbon  
96 (C) and  $0.13 \pm 0.03$  g N m<sup>-2</sup> d<sup>-1</sup> from the sediment (Amaro et al. 2010) and at PAP, *A. rosea* and  
97 *Ellipinion molle* Théel, 1879, together with other fauna removed the phytosterols from freshly  
98 deposited phytodetritus in less than four month (Ginger et al. 2001).

99  
100 Whereas holothurians alter the chemical composition of detritus in the sediment by depleting it  
101 for specific labile compounds, like sedimentary proteins (Amaro et al. 2010), this detritus  
102 composition also affects the species composition of holothurians (Wigham et al. 2003a;  
103 FitzGeorge-Balfour et al. 2010). At PAP, especially *A. rosea*, *P. diaphana* and *O. mutabilis*  
104 *mutabilis* had a high concentration of carotenoids in their ovaries which are important for the  
105 reproductive success of the species (Wigham et al. 2003b; Tsushima 2007; Svensson and Wong  
106 2011). Therefore, Wigham et al. (2003a) suggested that higher concentrations of carotenoids in  
107 the gonads of *A. rosea* as compared to other holothurians might give this species a reproductive  
108 advantage which could explain the so-called ‘Amperima’ event. During this event, the density of  
109 *A. rosea* increased by three orders of magnitude due to large-scale recruitment events that  
110 followed changes in the organic C flux to the abyssal plain, even though the total megafauna  
111 biomass did not change significantly (Bett et al. 2001; Billett et al. 2001, 2010). However, the  
112 input of fresh phytodetritus will change under climate change scenarios in the future and  
113 predictions say that it will rather decrease than increase (Smith et al. 2008; Wohlers et al. 2009;

114 Yool et al. 2017). Furthermore, warming temperatures and higher CO<sub>2</sub> partial pressures  
115 compared to current conditions likely lead to increasing degradation processes in the mid-water  
116 resulting in more degraded detritus reaching the deep-sea (Riebesell et al. 2007; Marsay et al.  
117 2015). Hence, it is important to know how dependent holothurians are on fresh phytodetritus  
118 compared to the detritus present in the sediment, especially for their amino acid and fatty acid  
119 demands.

120

121 Amino acids, the building blocks of proteins, are required to produce enzymes, structural tissue  
122 of fauna, and cell walls of bacteria (Phillips 1984; Libes 2009). Half of the 20 most common  
123 amino acids in faunal proteins can be synthesized by the organism itself (Phillips 1984), whereas  
124 the other half has to be taken up with the diet and are therefore called ‘essential’ amino acids  
125 (EAA) (Phillips 1984). Amino acids include ‘source amino acids’ (i.e., glycine, serine,  
126 phenylalanine, tyrosine, lysine), which preserve their  $\delta^{15}\text{N}$  values along the trophic chain because  
127 no new bonds are formed to the nitrogen (N) atom nor are bonds cleaved (McClelland and  
128 Montoya 2002; Chikaraishi et al. 2009). Other amino acids are ‘metabolic amino acids’ (i.e.,  
129 threonine) (Chikaraishi et al. 2009) and ‘trophic amino acids’ (i.e., asparagine, glutamine,  
130 alanine, isoleucine, leucine, valine, proline) (Chikaraishi et al. 2009). The  $\delta^{15}\text{N}$  values of ‘trophic  
131 amino acids’ become enriched during metabolic transamination when N bonds are cleaved  
132 (McClelland and Montoya 2002; Chikaraishi et al. 2009). The larger the difference between the  
133 ‘source amino acids’ and the ‘trophic amino acids’, the higher is the trophic level of an organism,  
134 so the ratio of the  $\delta^{15}\text{N}$  values of glutamic acid and phenylalanine has been used to estimate the  
135 trophic level of an organism following Chikaraishi et al. (2009).

136

137 Fatty acids, the main components of lipids, have several functions, such as serving as energy  
138 source (Lindsay 1975), being involved in the transduction of signals (Graber et al. 1994;  
139 Faergeman and Knudsen 1997), and gene expression (Sampath and Ntambi 2004), and being  
140 components of membranes (van Deenen 1966; Spector and Yorek 1985). They contain neutral-  
141 lipid-derived fatty acids (NLFAs; e.g., C16:1 $\omega$ 7, C16:3 $\omega$ 3, C20:1, C20:5 $\omega$ 3; Maier et al. 2019;  
142 Engel et al. 2023) and phospholipid-derived fatty acids (PLFAs; e.g., C16:0, C18:1 $\omega$ 9 *cis*,  
143 20:1 $\omega$ 9, 22:2 $\omega$ 6; Stratmann et al. 2022; Hoving et al. 2023) (Spector and Yorek 1985; Dalsgaard  
144 et al. 2003). NLFAs are required to build wax esters and the storage lipids triacylglycerols  
145 (Sargent and Falk-Petersen 1988; Ackman 1989), whereas PLFAs are necessary to build  
146 structural phospholipids of cell membranes (Spector and Yorek 1985). Fatty acids may be  
147 unsaturated or saturated, and generally a higher number of unsaturated bonds implies that the  
148 fatty acid is more labile than a fatty acid with fewer unsaturated bonds (Sargent 1995).  
149 ‘Essential’ fatty acids have to be taken up with the diet (Stubbs and Smith 1990) because they  
150 can generally only be synthesized *de novo* by primary producers (Sargent 1995). Since several  
151 fatty acids are transferred conservatively (i.e., untransformed) from primary producers and  
152 primary consumers to higher trophic levels (Lovern 1935), they may serve as trophic markers  
153 and inform about diets (Kharlamenko et al. 1995).

154

155 To decipher feeding types and diet preferences of holothurians and their ecological role in the  
156 Peru Basin, we combined stable isotope analyses of bulk tissue, gut content, and feces with  
157 compound-specific stable isotope analysis (CSIA) of amino acids and fatty acids. Furthermore,  
158 we performed a pulse-chase experiment with deep-sea holothurians that were fed *in-situ* with  $^{15}\text{N}$   
159 and  $^{13}\text{C}$ -enriched phytodetritus (*Skeletonema costatum* (Greville) Cleve, 1873) to compare how

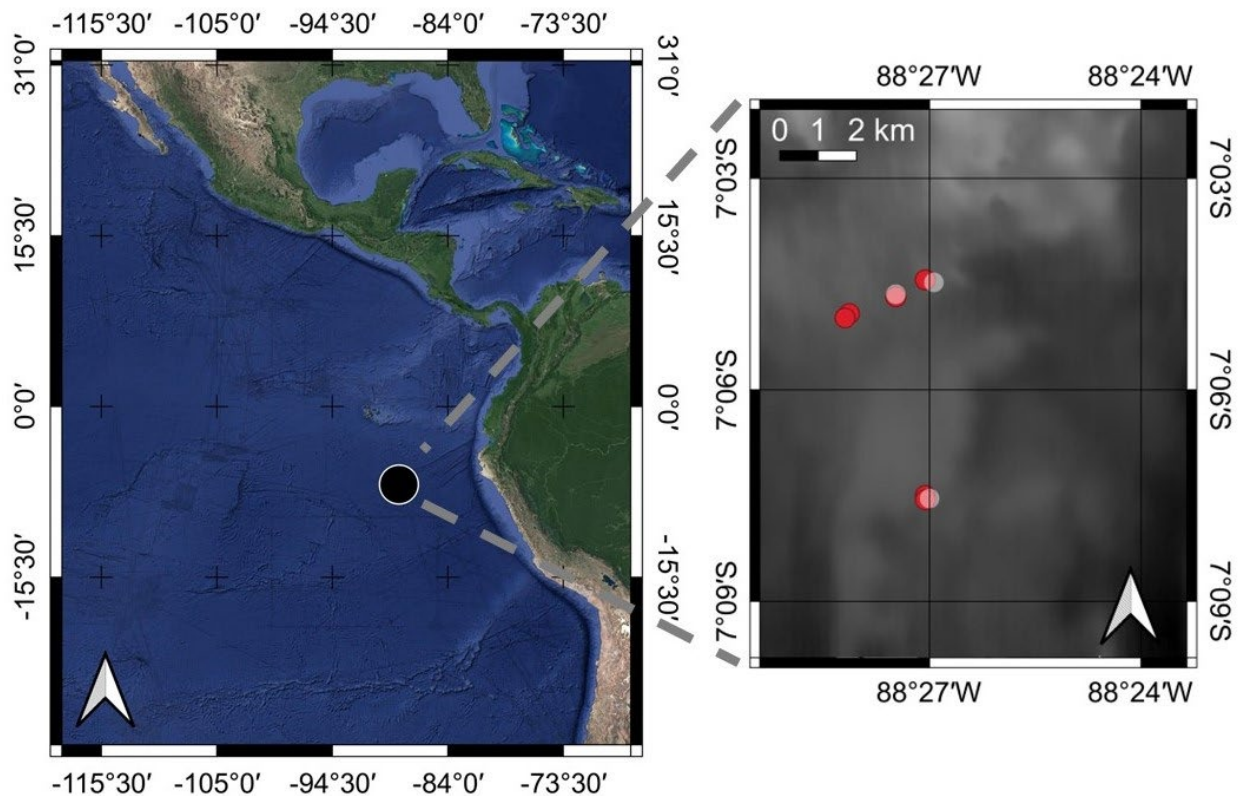
160 much of their daily amino acid and fatty acid demands holothurians can meet from ingesting  
161 sediment and which amino acids and fatty acids they have to extract from fresh phytodetritus.  
162 These two approaches allowed us to address the following research hypotheses 1) resource  
163 partitioning facilitates the high biodiversity of deposit-feeding holothurians in the Peru Basin, 2)  
164 holothurians reduce organic C availability in sediments of the Peru Basin, and 3) selective-  
165 feeding holothurians depend on amino acids and fatty acids from fresh phytodetritus.

## 166 Material and methods

### 167 Study site

168 The Peru Basin (Fig. 1) in the SE Pacific Ocean is a 4,000 to 4,400 m (Wiedicke and Weber  
169 1996) deep polymetallic nodule-rich abyssal plain covered with a 10 to 20 cm thick layer of  
170 brown fluffy sediment (Mevenkamp et al. 2019) of silty clay and clayey silt (Grupe et al. 2001)  
171 on which nodules lay with densities of  $18.1 \pm 11.3 \text{ kg m}^{-2}$  (Marchig et al. 2001). The sediment  
172 porosity is 0.93 (Vonnahme et al. 2020) and the top 1 cm of surface sediment contains  
173  $0.09 \mu\text{g ml}^{-1}$  chlorophyll-a and  $0.23 \mu\text{g ml}^{-1}$  phaeopigments (Vonnahme et al. 2020). The upper  
174 10 cm of sediment is fully oxygenated, and the oxygen penetrates the sediment down to 12 to  
175 20 cm sediment depth (Paul et al. 2018).

177



178 **Figure 1.** Location of the Peru Basin in the Pacific Ocean (left panel) with detailed positions of  
179 holothurian sampling sites (right panel; red symbols) and *in-situ* experiments (white transparent  
180 symbols) during RV *Sonne* cruise SO242-2 in September – October 2015. Bathymetry data of  
181 the right panel from is Gausepohl et al. (2019, 2020) and data from of the left panel is from  
182 Google Earth.

184 The water depth at the sampling stations ranged from 4136.3 to 4429.4 m.

185  
186  
187  
188  
189  
190  
191  
192  
193  
194  
195  
196  
197  
198  
199  
200  
201  
202  
203  
204  
205  
206  
207  
208  
209  
210  
211  
212  
213  
214  
215  
216  
217  
218  
219  
220  
221  
222  
223  
224  
225  
226  
227

### **Sampling of holothurians**

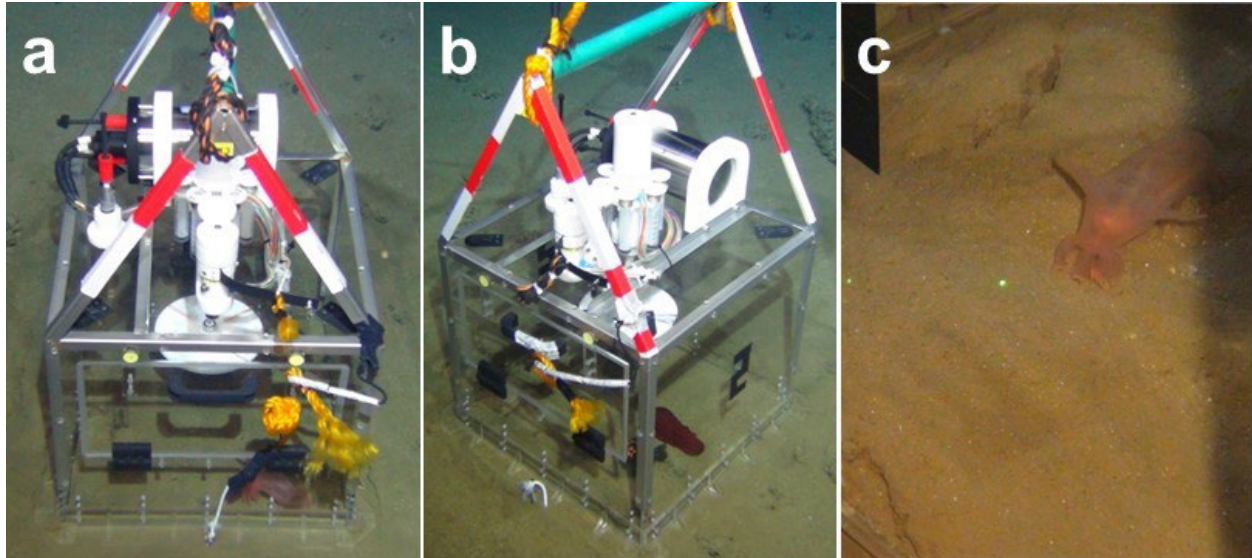
During “JPI Healthy and Productive Seas and Ocean” RV *Sonne* cruise SO242-2 to the Peru Basin in August and September 2015 (Boetius 2015), holothurians of the putative species Elpidiidae gen sp. Théel, 1882 (n = 1), *Amperima* sp. Pawson, 1965 (n = 4), *Benthodytes* sp. Théel, 1882 (n = 2), *Benthodytes typica* Théel, 1882 (n = 1), *Galatheathuria* sp. Hansen & Madsen, 1956 (n = 1), *Oneirophantha* sp. Théel, 1879 (n = 1), *Psychronaetes hanseni* Pawson, 1983 (n = 1), *P. longicauda* (n = 1), *Psychropotes semperiana* Théel, 1882 (n = 1), *Synallactes* sp. Ludwig, 1894 (morphotype “pink”; n = 1), and Synallactidae gen sp. Ludwig, 1894 (n = 2) were collected opportunistically with the suction sampler of the remotely operated vehicle (ROV) Kiel 6000 (Fig. 1, Table S1). As a result, sampling of several species was not balanced, but due to logistical constraints it was often limited to n = 1 or n = 2. Aboard RV *Sonne*, the specimens were dissected to separate the gut and its content from the remaining tissue. All samples were shock-frozen in liquid nitrogen and stored frozen at -20°C. Additionally, the putative holothurians species *Amperima* sp. (n = 3), *Benthodytes* sp. (n = 3), *B. typica* (n = 4), *Mesothuria* sp. Ludwig, 1894 (n = 1), *Peniagone* sp. Théel, 1882 (n = 1), and Synallactidae gen sp. (n = 1) from the study of Brown et al. (2018) were included in the analysis. These specimens were collected with the ROV suction sampler and transported to respiratory chambers to measure oxygen consumption of individual holothurian specimens over a period of 72 hours. Aboard RV *Sonne*, the holothurians specimens were shock-frozen intact in liquid nitrogen and stored at -21°C. Feces of holothurians that defecated inside the respiratory chambers were sampled and frozen at -21°C. Due to the very low *in-situ* temperatures (1.84 – 1.85°C; Brown et al. 2018), no changes in bulk and/ or compound-specific composition of the feces was expected.

### **Sampling of sediment**

Sediment samples were taken with ROV-deployed push cores and a benthic chamber lander system. After retrieval of push cores and the lander on board, the cores, and the lander chambers (484cm<sup>2</sup>) were sliced in two sediment intervals (0 – 2 cm and 2 – 5 cm sediment layers). Subsamples (35 ml) were taken from each sediment interval and stored frozen at -20°C.

### ***In-situ* experiment**

Pulse-chase *in-situ* experiments were performed during RV *Sonne* cruise SO242-2 by placing large (50 × 50 cm footprint) benthic incubation chambers (Stratmann et al. 2018a) over a single holothurian specimen at the seafloor (n = 6, putative species: *Amperima* sp., *Benthodytes* sp., *Peniagone* sp.) (Fig. 2) with ROV Kiel 6000. The holothurians were fed by injection of 0.5 g dry mass (DM) freeze-dried phytodetritus (i.e., *S. costatum*; equivalent to 40 mmol C m<sup>-2</sup> and 5 mmol N m<sup>-2</sup>) that was enriched in δ<sup>13</sup>C and δ<sup>15</sup>N (29 at% <sup>13</sup>C and 37 at% <sup>15</sup>N) into the chamber. After 3 d of incubation, the experiment was terminated, and the holothurians were collected via the suction pump of the ROV Kiel 6000. Aboard the vessel, the holothurians were dissected to separate the gut and its content from the remaining tissue. All samples were flash-frozen in liquid nitrogen and stored frozen at -20°C.



228  
 229 **Figure 2.** Incubation of (a) *Amperima* sp., (b) *Benthodytes* sp., and (c) *Peniagone* sp. inside the  
 230 benthic incubation chamber during the *in-situ* pulse-chase experiments at the Peru Basin at  
 231 ~4,100 m water depth. Photos by ROV Kiel 6000 (GEOMAR, Germany).

232  
 233 **Laboratory analyses**

234 **Bulk analyses**

235 In the shore-based laboratory at NIOZ-EDS (Yerseke, Netherlands), the samples were freeze-  
 236 dried and finely-ground with mortar and pestle. Total C (TC)/  $\delta^{13}\text{C}$  and total N (TN)/  $\delta^{15}\text{N}$   
 237 content of the holothurian body wall tissue was measured in not acidified samples and organic C  
 238 (org. C)/  $\delta^{13}\text{C}$  was measured in acidified tissue samples with a Thermo Flash EA 1112 elemental  
 239 analyzer (EA; Thermo Fisher Scientific, USA) which was coupled to a DELTA V Advantage  
 240 Isotope Ratio Mass Spectrometer (IRMS; Thermo Fisher Scientific, USA). Org. C/  $\delta^{13}\text{C}$ , and  
 241 TN/  $\delta^{15}\text{N}$  contents of acidified holothurian gut contents, feces, and sediment were measured with  
 242 the same EA-IRMS and the  $\delta^{13}\text{C}$  and  $\delta^{15}\text{N}$  data were normalized against L-glutamic acid isotope  
 243 reference material USGS40 (Qui et al. 2004) and USGS41a (Qi et al. 2016) following Sharp  
 244 (2017). Stable isotope values are presented in  $\delta$  notation relative to Vienna Pee Dee Belemnite  
 245 for  $\delta^{13}\text{C}$  and relative to air for  $\delta^{15}\text{N}$ .

246 Sediment grain size of holothurian gut content was determined by laser diffraction on freeze-  
 247 dried and sieved (<1 mm) sediment samples in a Malvern Mastersizer 2000.

248  
 249 **Analysis of amino acids**

250 Hydrolysable amino acids (HAA) from holothurian body wall tissue and phytodetritus were  
 251 extracted following a modified protocol of Veuger et al. (2005): Briefly, HAAs in holothurian  
 252 tissue and HAAs in phytodetritus were hydrolyzed by adding 0.01 to 0.02 g freeze-dried finely  
 253 ground holothurian tissue and 0.01 to 0.02 g phytodetritus, respectively, to 1.5 ml 6 M HCl in  
 254 10 ml screw-cap vials. A  $\text{N}_2$ -headspace was created in the vials by flushing with  $\text{N}_2$ -gas for  
 255 10 sec before the vials were closed and heated for 20 h at 110°C. After cooling, 10  $\mu\text{l}$  internal L-  
 256 Norleucine standard per mg dry faunal tissue (stock solution: 2.5  $\text{mg mL}^{-1}$  L-Norleucine  
 257 acidified with 100  $\mu\text{l}$  12 M HCl) was added and the solution was evaporated under  $\text{N}_2$ -flow at  
 258 60°C. HAAs from holothurian tissue were derivatized by adding 0.5 ml acidified propan-2-ol to  
 259 the sample and by heating the closed vials at 110°C for 90 min. Afterwards, the vials were

260 cooled down and the solution was evaporated under N<sub>2</sub>-flow at 50°C. After evaporating all  
261 solution, 200 µl dichloromethane (DCM) was added and the solution was evaporated again.  
262 When the samples were dry, 150 µl DCM and 50 µl pentafluoropropionic anhydride were added,  
263 the vials were closed and heated for 10 min at 110°C. The solvent was extracted by adding  
264 0.5 mL chloroform and 1 ml phosphorus-buffer to the sample, shaking it until the lower  
265 chloroform fraction was clear and centrifuging the vials with 2,000 rpm for 10 min. The  
266 chloroform fraction was transferred to GC vials and evaporated again. When the sample was  
267 completely dry, it was dissolved in ethyl acetate. Concentrations (µg C g<sup>-1</sup> dry mass DM  
268 holothurian body wall tissue), and δ<sup>13</sup>C (‰) and δ<sup>15</sup>N (‰) of HAAs were measured with a HP  
269 6890 gas chromatograph (Hewlett Packard/ Agilent, USA) coupled with a DELTA-Plus Isotope  
270 Ratio Mass Spectrometer (Thermo Fisher Scientific, USA) on a polar analytical column (ZB5-  
271 5MS; 60m length, 0.32mm diameter, 0.25µm film thickness; Phenomenex, USA). The  
272 concentrations of amino acids were determined using L-Norleucine as internal standard and δ<sup>13</sup>C  
273 and δ<sup>15</sup>N data of amino acids were standardized against L-Norleucine which had δ<sup>13</sup>C and δ<sup>15</sup>N  
274 values of -31.31 ± 0.14 ‰ and -4.45 ± 0.05 ‰, respectively, as determined by EA-IRMS prior to  
275 its application as internal standard.  
276 Following Veuger et al. (2005), individual HAAs were identified based on their retention time in  
277 relation to the L-Norleucine standard. Asparagine *and* aspartic acids, and glutamine *and* glutamic  
278 acid, however, were reported as sums, because during the hydrolysis asparagine is converted to  
279 aspartic acid and glutamine to glutamic acid (Uhle et al. 1997; Erbe 1999). Except for histidine,  
280 cysteine, tryptophan, and arginine, all other 20 “common” HHA can be detected with this  
281 method (Erbe 1999), but the recovery of methionine can be ~30% (Maier et al. 2019). Therefore,  
282 methionine was excluded from the analysis. C concentrations were also corrected for the C-  
283 atoms added during the derivatization step.

284

### 285 **Analysis of fatty acids**

286 Lipids were extracted from holothurian body wall tissue, phytodetritus, feces, and gut content  
287 following a modified Bligh and Dyer extraction method (Bligh and Dyer 1959; Boschker 2008).  
288 Freeze-dried, homogenized powder of holothurian tissue (~50 – 150 mg), phytodetritus (~1 mg),  
289 feces and gut content (~150 mg – 2.0 g) were mixed with 6 ml MilliQ-water 15 ml methanol  
290 (HPLC grade, 99.8%), and 7.5% chloroform (HPLC grade, 99.5%) in pre-cleaned test tubes. The  
291 tubes were shaken for 2 h, before 7.5 ml chloroform were added, and the tubes were shaken  
292 again. 7.5 ml MilliQ-water were added, and the tubes were stored at -21°C for 12 h for  
293 separation of the solvent layers. The lower solvent layer contained the lipid extract dissolved in  
294 chloroform and was transferred to pre-weighted test tubes. After determining the weight of the  
295 chloroform extract, it was fractionated into the different fatty acid classes over an activated  
296 silicic acid column (heated at 120°C for 2 h; Merck Kieselgel 60) via eluting with 7 ml  
297 chloroform, 7 ml acetone, and 15 ml methanol. The acetone fraction was discarded, whereas the  
298 chloroform fraction containing the NLFAs and the methanol fraction with the PLFAs were  
299 collected in separate test tubes and evaporated to dryness.  
300 PLFAs and NLFAs were derivatized to fatty acid methyl esters (FAMES) by adding 1 ml  
301 methanol-toluene mix (1:1 volume/ volume), 20 µl of an internal standard (1 mg C19:0  
302 FAME mL<sup>-1</sup>), and 1 ml 0.2 M methanolic NaOH to the test tubes with the PLFAs and NLFAs  
303 extracts. After an incubation at 37°C for 15 min, 2 ml *n*-hexane, 0.3 ml 1 M acetic acid, and 2 ml  
304 MilliQ-water were added. The solution was mixed very well and when the layers had separated,  
305 the (top) *n*-hexane layer was transferred to new test tubes. Additional 2 ml *n*-hexane were added

306 to the previously used test tubes that contained the acetic acid-MilliQ-water solution, and the  
 307 step was repeated. The *n*-hexane layer was transferred again to the new test tubes and 20  $\mu$ l of a  
 308 second internal standard (1 mg C12:0 FAME mL<sup>-1</sup>) were added. *n*-hexane was evaporated  
 309 completely, and the FAMEs dissolved in 200  $\mu$ l *n*-hexane were transferred to measuring vials.  
 310 The FAMEs from holothurian tissues and phytodetritus were separated on a very polar BPX70  
 311 column (50 m length, 0.32 mm inner diameter, 0.25  $\mu$ m film thickness; SGE Analytical Science)  
 312 with a HP 6890 GC (Hewlett Packard/ Agilent, USA). The FAMEs from sediment, feces, and gut  
 313 content were separated on a polar ZB5-5MS column (60 m length, 0.32 mm diameter, 0.25  $\mu$ m  
 314 film thickness; Phenomenex, USA) on the same GC. Concentrations ( $\mu$ g C g<sup>-1</sup> DM holothurian  
 315 body wall tissue) and  $\delta^{13}\text{C}$  values (‰) of FAMEs in holothurian body wall tissue, feces, and gut  
 316 content were measured on a Finnigan Delta Plus IRMS (Thermo Fisher Scientific, USA) coupled  
 317 to the GC via a combustion GC-c-III interface (Thermo Fisher Scientific, USA). Five reference  
 318 material FAMEs (C14:0 FAME, C16:0 FAME, C18:0 FAME, C20:0 FAME, C24:0 FAME) from  
 319 Schimmelmann Research (Indiana University Bloomington, USA) were combined in a mix and  
 320 served as standard against which the  $\delta^{13}\text{C}$  and  $\delta^{15}\text{N}$  data were normalized following (Sharp  
 321 2017).

322 The peaks of FAMEs in the chromatograms were identified as specific fatty acids based on their  
 323 retention time in relation to the internal standards C12:0 FAME and C19:0 FAME, and the  
 324 omnipresent peak of C16:0 following Boschker et al. (1999). The retention times of certified  
 325 reference FAME standards from Sigma-Aldrich (USA; product numbers: L-7272, T-0627, M-  
 326 3378, P-6250, P-5177, H-4515, S-5376, N-5377, A-3881, P-9667, P-0203, E-4762, B-3271, T-  
 327 9900, L-6766, -4754), from Larodan (Sweden; product numbers: 20-1603-4, 20-1812-9, 20-  
 328 1802-13, 20-1840-4, 20-2004-7, 20-2003-9, 20-2205-9, 90-1100, 90-1051, 90-1054, 21-1610-7,  
 329 21-1710-7, 21-1810-7, 21-1413-7, 21-1615-7, 11-1412-7), from Supelco® Analytical (USA;  
 330 product numbers: Supelco 47033, Supelco-47033, Supelco-47015-U, Supelco-47085-U,  
 331 Supelco-47080-U), and from Schimmelmann Research (fatty acid mixture F8-4) measured on the  
 332 same GC columns served as references. Further peaks in the chromatograms were confirmed by  
 333 gas chromatography/mass spectrometry (GC/MS) following Kurkiewicz et al. (2003). Whenever,  
 334 the identification of chromatogram peaks was not unique, because fatty acids co-eluted, both  
 335 fatty acids were reported as “fatty acid 1/ fatty acid 2”.

336 C concentrations were calculated based on peak area of the chromatogram peaks using the two  
 337 internal standards (C12:0 FAME and C19:0 FAME) for area correction and corrected for the C-  
 338 atoms added during the derivatization step.

339 A list with of dominant fatty biomarkers is presented in Table 1.

340

341 **Table 1.** Fatty acids used as biomarkers of potential food sources of holothurians from the Peru  
 342 Basin.

343 Abbreviations: ARA = arachidonic acid (C20:4 $\omega$ 6), DHA = docosahexaenoic acid (C22:6 $\omega$ 3),

344 EPA = eicosapentaenoic acid (C20:5 $\omega$ 3).

| Fatty acid       | Main sources of fatty acid                     | Reference            |
|------------------|--|----------------------|
| Organic matter   |  |                      |
| C18:1 $\omega$ 9 | Highly degraded carrion-derived organic matter | (Graeve et al. 2001) |
| Bacteria         |  |                      |

|  |   |   |
|--|---|---|
| <i>i</i> -C14:0, <i>i</i> -C15:0, <i>ai</i> -C15:0, <i>i</i> -C16:0, and C18:1 $\omega$ 7 <i>cis</i> ;<br>C18:2 $\omega$ 6       | Marine bacteria; gram-positive bacteria; piezotolerant bacteria   | (Findlay et al. 1990; Middelburg et al. 2000; Wang et al. 2014)   |
| 10-Me-C16:0, <i>ai</i> -C17:0, <i>i</i> -C17:0, and <i>cy</i> -C17:0<br>C16:1 $\omega$ 5<br>C16:1 $\omega$ 7<br>C16:1 $\omega$ 9 | Sulfate-reducing and other anaerobic bacteria<br>Desulfobacteraceae bacteria<br>Bacteria in fish intestines<br>Deep-water/ benthic bacteria | (Findlay et al. 1990)<br>(Elvert et al. 2003)<br>(Yano et al. 1997)<br>(Zhao et al. 2015; Choi et al. 2015) |
| <b>Primary producers</b>   |   |   |
| C16:4 $\omega$ 1, C16:1 $\omega$ 7, and EPA;<br>$\frac{C16:1\omega7}{C16:0} > 1$ or $\frac{DHA}{EPA} < 1$                        | Diatoms   | (Kharlamenko et al. 1995; Budge and Parrish 1998; Dalsgaard et al. 2003; Parrish et al. 2005)               |
| C18:4 $\omega$ 3 and DHA;<br>$\frac{C16:1\omega7}{C16:0} < 1$ or $\frac{DHA}{EPA} > 1$   | Dinoflagellates   | (Budge and Parrish 1998; Dalsgaard et al. 2003; Parrish et al. 2005)  |
| <b>Consumers</b>   |   |   |
| C20:1 $\omega$ 9, C22:1 $\omega$ 11  | Calanoid copepods   | (Falk-Petersen et al. 1987; Dalsgaard et al. 2003)  |
| ARA; C22:5 $\omega$ 5;<br>$\frac{EPA}{ARA}$ -ratio   | Agglutinated foraminifera   | (Larkin et al. 2014; Kharlamenko 2018)  |

345

**Data analyses****Concentration factors**

348 To examine the degree to which PLFAs were concentrated between surface sediment (0 – 2cm  
349 layer) and gut content and feces, a concentration factor  $CF$  was calculated:

$$350 CF_{gut\ content} = \frac{[gut\ content_{PLFA}]}{[sediment_{PLFA}]}, \quad (1)$$

$$351 CF_{feces} = \frac{[feces_{PLFA}]}{[sediment_{PLFA}]}, \quad (2)$$

352 where  $[gut\ content_{PLFA}]$  corresponds to the total PLFA concentration in gut content,  $[feces_{PLFA}]$   
353 to the total PLFA concentration in feces, and  $[sediment_{PLFA}]$  to the mean total PLFA  
354 concentration in surface sediment.

355

**Trophic levels**

357 Trophic levels ( $TL$ ) of holothurian species were calculated following Chikaraishi et al. (2009) as

$$358 TL = \frac{(\delta^{15}N_{Glu} - \delta^{15}N_{Phe} - \beta)}{\Delta_{Glu-Phe}} + 1 = \frac{(\delta^{15}N_{Glu} - \delta^{15}N_{Phe} - 3.4)}{7.6} + 1. \quad (3)$$

359  $\delta^{15}N_{Glu}$  is the  $\delta^{15}N$  of the amino acid glutamic acid (‰) and  $\delta^{15}N_{Phe}$  corresponds to the  $\delta^{15}N$  of  
360 the amino acid phenylalanine (‰).  $\beta$  is the fractionation between glutamic acid and  
361 phenylalanine at trophic level 1 and  $\Delta_{Glu-Phe}$  is the  $^{15}N$  enrichment in glutamic acid relative to  
362 phenylalanine.

363 Two holothurian species are considered to have two different trophic levels when the difference  
 364 in trophic levels between two species is  $> \pm 0.44$ . This value corresponds to the mean standard  
 365 deviation of the calculated trophic level ( $\sigma_{TL}$ ; propagation of error) across all holothurians that  
 366 was determined following equation S4 in (Jarman et al. 2017) as:

$$367 \sigma_{TP} = \sqrt{\left(\frac{1}{\Delta_{Glu-Phe}}\right)^2 \sigma_{\delta^{15}N_{Glu}}^2 + \left(\frac{-1}{\Delta_{Glu-Phe}}\right)^2 \sigma_{\delta^{15}N_{Phe}}^2 + \left(\frac{1}{\Delta_{Glu-Phe}}\right)^2 \sigma_{\beta}^2 + \left(\frac{-1}{\Delta_{Glu-Phe}^2} (\delta^{15}N_{Glu} - \delta^{15}N_{Phe} + \beta)\right)^2 \sigma_{\Delta_{Glu-Phe}}^2}, \quad (4)$$

368 where  $\sigma_{\beta}$  is 0.9‰,  $\sigma_{\Delta}$  is 1.1‰, and  $\beta$  is the fractionation between glutamic acid and phenylalanine  
 369 (Jarman et al. 2017).

370

### 371 Heterotrophic re-synthesis of amino acids

372 Total heterotrophic re-synthesis of amino acids ( $\sum V$ ) was approximated as the sum of variance  
 373 of individual  $\delta^{15}N$  values of the trophic amino acid alanine, aspartic acid, glutamic acid, leucine,  
 374 and proline (McCarthy et al. 2007):

$$375 \sum V = \sum_1^n |x_{amino\ acid} - \bar{x}_{amino\ acid}| \quad (5)$$

376  $x$  symbolized each trophic amino acids'  $\delta^{15}N$  value,  $\bar{x}$  is the mean trophic amino acids'  $\delta^{15}N$   
 377 value and  $n$  is the total number of trophic amino acids used in this calculation (McCarthy et al.  
 378 2007).

379

### 380 Bayesian mixing model

381 The relative contribution of potential food sources (Table 2) to the diets of the different  
 382 holothurian species (i.e., consumers) was estimated using Bayesian mixing models based on the  
 383 natural abundance stable isotopic composition ( $\delta^{13}C$ ,  $\delta^{15}N$ ) of food sources and holothurians.

384

385 **Table 2:** Stable isotopic composition of potential food sources of holothurians used in the  
 386 Bayesian mixing model.

| Food source                     | $\delta^{13}C$ (‰) | $\delta^{15}N$ (‰) | n  | Reference                   |
|---------------------------------|--------------------|--------------------|----|-----------------------------|
| Bulk sediment                   | $-20.7 \pm 0.6$    | $10.3 \pm 2.0$     | 4  | This study                  |
| Diatom-derived<br>phytodetritus | $-12.8 \pm 0.2$    | $1.9 \pm 0.3$      | 3  | Unpublished data            |
| Heterotrophic<br>prokaryotes    | $-15.6 \pm 1.5$    | $2.4 \pm 1.4$      | 4  | (Pagès et al. 2014)         |
| Foraminifera                    | $-19.2 \pm 0.5$    | $8.7 \pm 1.3$      | 33 | (Nomaki et al. 2008)        |
| Fungi                           | $-25.8 \pm 0.6$    | $0.9 \pm 1.6$      | 12 | (Gutiérrez et al.<br>2020)  |
| Nematoda                        | $-19.3 \pm 0.4$    | $6.5 \pm 5.8$      | 3  | (Stratmann et al.<br>2018a) |

387

388 The Bayesian analysis was conducted using the *R* (version 4.3.0; R-Core Team 2022) package  
 389 *rjags* (version 4.3.1; Stock et al. 2020) and the mixing models were performed using the *R*  
 390 package *MixSIAR* (version 3.1.12; Stock et al. 2018, 2020). A general trophic enrichment factor  
 391 of 0.5‰ for C and 3.4‰ for N (Fry 2006) was applied for all food sources. The mixing models  
 392 for the fixed factor 'species' were fitted using the Markov Chain Monte Carlo (MCMC) method  
 393 on 300,000 iterations for informative priors (i.e.,  $\alpha = (1, 1, 1, 0.5, 0.5, 0.5)$  for sedimentary

394 detritus, phytodetritus, heterotrophic prokaryotes, Foraminifera, Fungi, and Nematoda,  
 395 respectively). Model convergence was diagnosed with Gelman-Rubin diagnostics  $\hat{R}$  ( $\hat{R} < 1.05$ )  
 396 (Gelman and Rubin 1992; Gelman et al. 2014; Roy 2020) and Geweke diagnostics  $Z_n$  (Geweke  
 397 1991; Roy 2020) being similar in all three chains. The model solutions are presented as mean  
 398 (%) with 95% and 75% Bayesian credibility intervals (BCI).

### 400 Cluster analysis of Sørensen–Dice coefficient $\beta_{sor}$

401 The Sørensen–Dice coefficient  $\beta_{sor}$  (Dice 1945; Sørensen 1948; Koleff et al. 2003) was  
 402 calculated using the ‘betadiver’ function in the R package *vegan* (version 2.6-2; Oksanen et al.  
 403 2017) to compare holothurian species based on their trophic levels ( $TL$ ), levels of heterotrophic  
 404 re-synthesis of amino acids ( $\sum V$ ), feeding selectivity based on concentration factor ( $CF$ ), and  
 405 food sources/ diet. For this purpose, the quantitative data  $TL$  and  $\sum V$  were first converted into  
 406 categories (Table 3) and then converted into binary (presence/ absence) data. The categorical  
 407 data ‘feeding selectivity’ (Table 3) and ‘food/sources diet’ were also converted into binary data.  
 408 Subsequently,  $\beta_{sor}$  was clustered by average linkage clustering (unweighted pair-group method  
 409 using arithmetic averages, UPGMA; Romesburg 1984) using the ‘hclust’ function in R. The  
 410 optimal number of clusters was identified by finding a consensus among the results of 20  
 411 different clustering algorithms using the ‘n\_clusters’ function in the R package *parameter*  
 412 (version 0.21.1; Lüdecke et al. 2020). The dendrogram was prepared with R package *factoextra*  
 413 (version 1.0.7; Kassambara and Mundt 2020).

414  
 415 **Table 3.** Parameters used to calculate the Sørensen–Dice coefficient  $\beta_{sor}$  presented as  
 416 quantitative data (ranges) and categorical data. ‘Food sources/ diet’ includes a list of the main  
 417 food sources of the investigated holothurian species which were identified by amino acid and  
 418 fatty acid analysis.

| Parameter  | Quantitative data   | Categorical data   |
|--|---------------------|--|
| Trophic level ( $TL$ )   | $TL = 2.0-2.5$      | $TL_{\text{group 1}}$  |
|  | $TL = >2.5-3.0$     | $TL_{\text{group 2}}$  |
|  | $TL = >3.0-3.5$     | $TL_{\text{group 3}}$  |
| Levels of heterotrophic re-synthesis of amino acids ( $\sum V$ ) | $\sum V = 0-1.5$    | $\sum V_{\text{group 1}}$  |
|  | $\sum V = >1.5-3.0$ | $\sum V_{\text{group 2}}$  |
|  | $\sum V = >3.0-4.5$ | $\sum V_{\text{group 3}}$  |
|  | $\sum V = >4.5-6.0$ | $\sum V_{\text{group 4}}$  |
|  | $\sum V = >6.0-7.5$ | $\sum V_{\text{group 5}}$  |
| Feeding selectivity based on concentration factor $CF$           | $CF = 0-10$         | no selectivity   |
|  | $CF = >10-50$       | selective  |
|  | $CF = >50-150$      | very selective   |
|  | $CF = >150$         | extremely selective  |
| Food sources/ diet   |                     | <ul style="list-style-type: none"> <li>– diatom-derived phytodetritus</li> <li>– dinoflagellate-derived phytodetritus</li> <li>– secondary consumer of detritus</li> <li>– sedimentary detritus</li> <li>– Foraminifera</li> <li>– bacteria</li> </ul> |

419

## 420 <sup>13</sup>C and <sup>15</sup>N incorporation

421 The bulk incorporations of phytodetritus C and N into holothurian body wall tissue and the  
422 incorporation of <sup>13</sup>C and <sup>15</sup>N into holothurian HAAs, PLFAs, and NLFAs were calculated as  
423 follows:

$$424 R_{bulk\ tissue, HAA, PLFA, NLFA} = \left( \frac{\delta^{13}C}{1000} + 1 \right) \times R_{standard}, \quad (6)$$

$$425 \text{ or } R_{bulk\ tissue, HAA, PLFA, NLFA} = \left( \frac{\delta^{15}N}{1000} + 1 \right) \times R_{standard} \quad (7)$$

426 where  $R_{standard}$  is 0.0111802 in case of C and  $R_{standard}$  is 0.0036782 in case of N. The fractions ( $F$ )  
427 of the <sup>13</sup>C and <sup>15</sup>N isotopes in the enriched tissue and HAAs, PLFAs, NLFAs ( $F_{sample}$ ) and  
428 background tissue (i.e., *Amperima* sp., *Benthodytes* sp., *Peniagone* sp. specimens collected in  
429 “Sampling of holothurians”) and HAAs, PLFAs, NLFAs ( $F_{background}$ ) were calculated as:

$$430 F = \frac{{}^{13}C}{({}^{13}C + {}^{12}C)} = \frac{R}{(R+1)} \quad (8)$$

$$431 \text{ or } F = \frac{{}^{15}N}{({}^{15}N + {}^{14}N)} = \frac{R}{(R+1)} \quad (9)$$

432 Subsequently, the incorporations of phytodetritus C and N ( $I$ ) in the tissue were calculated as:

$$433 I = \frac{(F_{sample} - F_{background}) \times total\ C}{phytodetritus\ enrichment} \quad (10)$$

$$434 \text{ or } I = \frac{(F_{sample} - F_{background}) \times total\ N}{phytodetritus\ enrichment} \quad (11)$$

435  
436 The incorporations of <sup>13</sup>C and <sup>15</sup>C in HAAs, PLFAs, NLFAs were calculated as:

$$437 I = (F_{sample} - F_{background}) \times total\ C \quad (12)$$

$$438 \text{ or } I = (F_{sample} - F_{background}) \times total\ N \quad (13)$$

439 For the calculation of <sup>13</sup>C incorporation into PLFAs and NLFAs, only PLFAs and NLFAs were  
440 considered that were present in at least four out of five samples.

441

## 442 Statistical analysis

443 To test whether the proportions of individual amino acids and fatty acids to total amino acids and  
444 fatty acids in (i) sediments compared to holothurians with natural abundance stable isotope  
445 composition and in (ii) phytodetritus compared to holothurians in the pulse-chase experiment  
446 were statistically significantly different (level of significance:  $\alpha = 0.05$ ), Wilcoxon Rank Sum  
447 Test  $W$  (also known as Mann Whitney U Test) was performed. This test allows to compare  
448 means of two different samples that are not normally distributed.

449

450 All data are presented as mean  $\pm$  1 standard deviation (SD). A list with the number of replicates  
451 per specific parameter and holothurian species is presented in Table S2.

452

## 453 Results

### 454 Chemical composition of sediment

455 Sediment in the Peru Basin consisted of  $0.63 \pm 0.01\%$  org. C in the upper 2 cm of sediment  
456 ( $n = 4$ ) and  $0.62 \pm 0.03\%$  org. C in the 2 to 5 cm sediment depth layer ( $n = 4$ ). TN content in  
457 each sediment layer was  $0.13 \pm 1.98 \times 10^{-3}\%$  N and the C/N ratios were  $5.44 \pm 0.02$  (0 – 2 cm)  
458 and  $5.45 \pm 0.19$  (2 – 5 cm). The sediment had  $\delta^{13}C$ -values of  $-20.7 \pm 0.6\%$  (0 – 2 cm;  $n = 4$ ) and  
459  $-21.8 \pm 1.2\%$  (2 – 5 cm;  $n = 4$ ), and  $\delta^{15}N$ -values of  $10.3 \pm 2.0\%$  (0 – 2 cm;  $n = 4$ ) and  
460  $8.20 \pm 0.8\%$  (2 – 5 cm;  $n = 4$ ).

461 The surface sediment layer (0 – 2 cm; n = 4) contained  $18.5 \pm 7.16 \mu\text{mol HAA g}^{-1}$  dry mass  
462 (DM) sediment, whereas the 2 to 5 cm layer (n = 4) had  $18.6 \pm 5.73 \mu\text{mol HAA g}^{-1}$  DM  
463 sediment. Alanine, glycine, and isoleucine contributed between  $51.0 \pm 2.28\%$  (0 – 2 cm; n = 4)  
464 and  $52.8 \pm 3.82\%$  (2 – 5 cm; n = 4) to the HAA concentration.

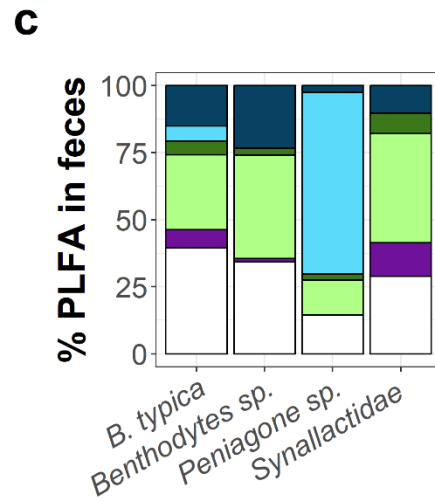
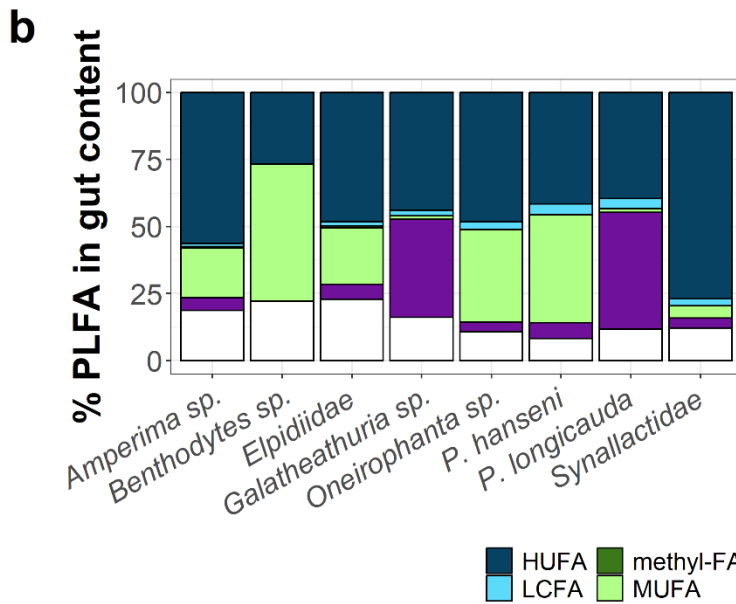
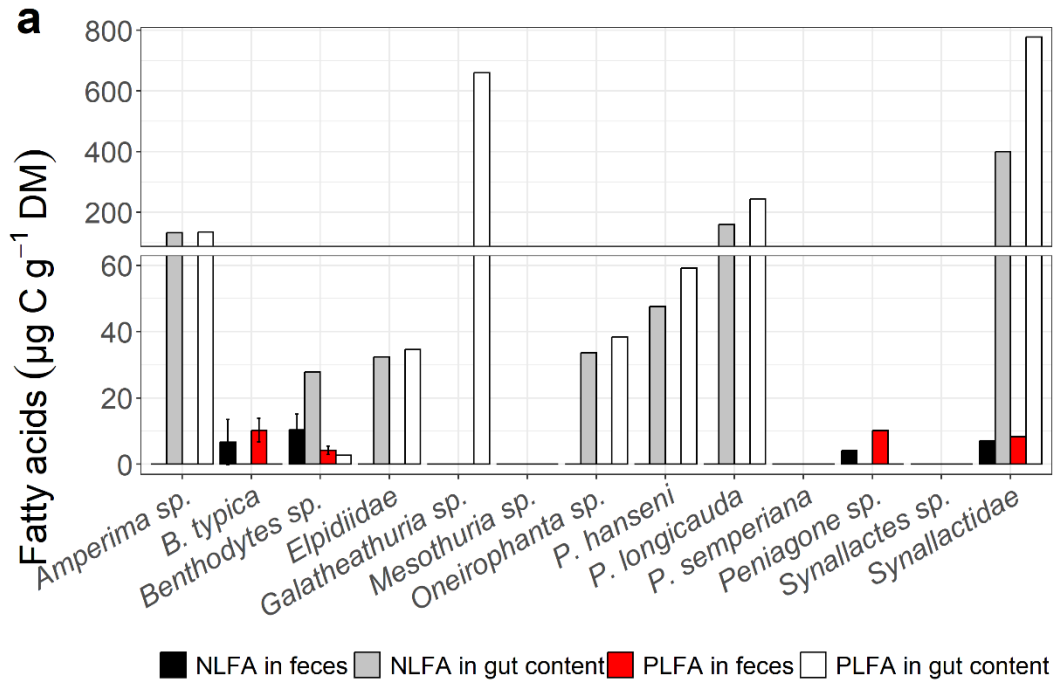
465 The surface sediment layer (0 – 2 cm; n = 3) contained  $0.19 \pm 0.04 \mu\text{mol C-PLFA g}^{-1}$  DM  
466 sediment, whereas the 2 to 5 cm layer (n = 3) had  $0.15 \pm 0.08 \mu\text{mol C-PLFA g}^{-1}$  DM sediment.  
467 The PLFAs C16:0, C16:1 $\omega$ 7 *cis*, and 18:1 $\omega$ 7 *cis*/ 18:1 $\omega$ 9 *trans* contributed  $34.9 \pm 11.1\%$   
468 (2 – 5 cm; n = 3) to  $44.4 \pm 3.16\%$  (0 – 2 cm; n = 3) to the total PLFA concentration in the  
469 respective sediment layers.

470

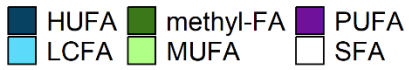
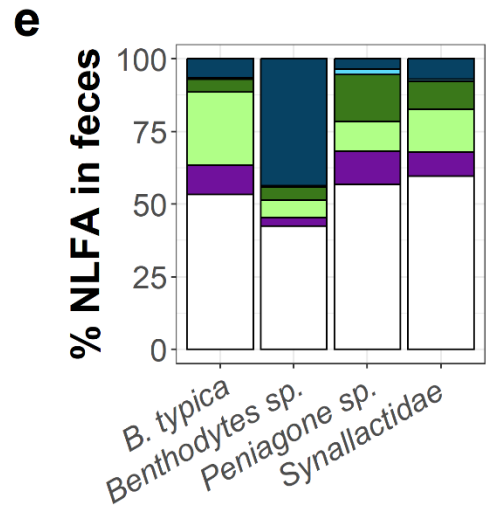
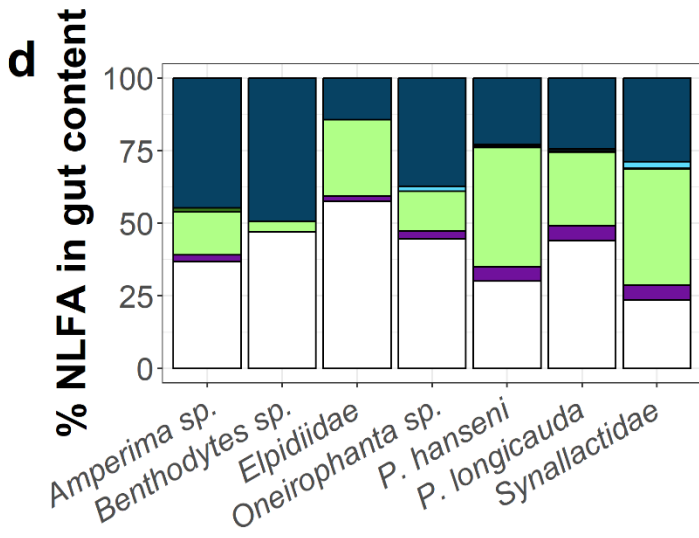
#### 471 **Gut content and feces of holothurians**

472 Gut contents of holothurians in the Peru Basin weighed  $1.93 \pm 3.56$  g DM gut content and ranged  
473 from 0.11 g DM gut content for *Peniagone* sp. to 12.5 g DM gut content for *P. hansenii*  
474 (Table 4). Org. C and TN contents of the gut content of all investigated holothurian specimens  
475 were  $5.34 \pm 4.13\%$  and  $1.04 \pm 0.87\%$ , respectively, and it contained  $244 \pm 304 \mu\text{g C-PLFA g}^{-1}$   
476 DM gut content and  $83.3 \pm 124 \mu\text{g C-NLFA g}^{-1}$  DM gut content (Fig. 3a). The concentration  
477 factor  $CF_{\text{gut content}}$  for PLFAs in holothurian gut content was on average  $105 \pm 131$  and ranged  
478 from 1.17 to 335 for *Benthodytes* sp. and Synallactidae gen sp., respectively (Table 4). The mean  
479 eicosapentaenoic acid (EPA, C20:5 $\omega$ 3)/ arachidonic acid (ARA, C20:4 $\omega$ 6)-ratio for gut content  
480 across all holothurians was  $3.20 \pm 5.58$ , the mean docosahexaenoic acid (DHA, C22:6 $\omega$ 3)/EPA-  
481 ratio was  $0.62 \pm 0.68$ , and the mean C16:1 $\omega$ 7/C16:0-ratio was  $0.81 \pm 0.85$  (Fig. 4a).

482



483  
 484 **Figure 3.** (a) Concentrations ( $\mu\text{g C g}^{-1} \text{ DM C}$ ) of phospholipid-derived fatty acids (PLFA) and  
 485 neutral-lipid-derived fatty acid (NLFA) in holothurian gut content and feces and the contribution  
 486 (%) of individual (b, c) PLFA classes and (d, e) NLFA classes to the total concentrations. Error  
 487 bars in (a) indicate 1 SD.  
 488 Abbreviations: HUFA = highly unsaturated fatty acid, LCFA = long-chain fatty acid, MUFA =  
 489 monounsaturated fatty acid, PUFA = polyunsaturated fatty acid, SFA = saturated fatty acid.  
 490



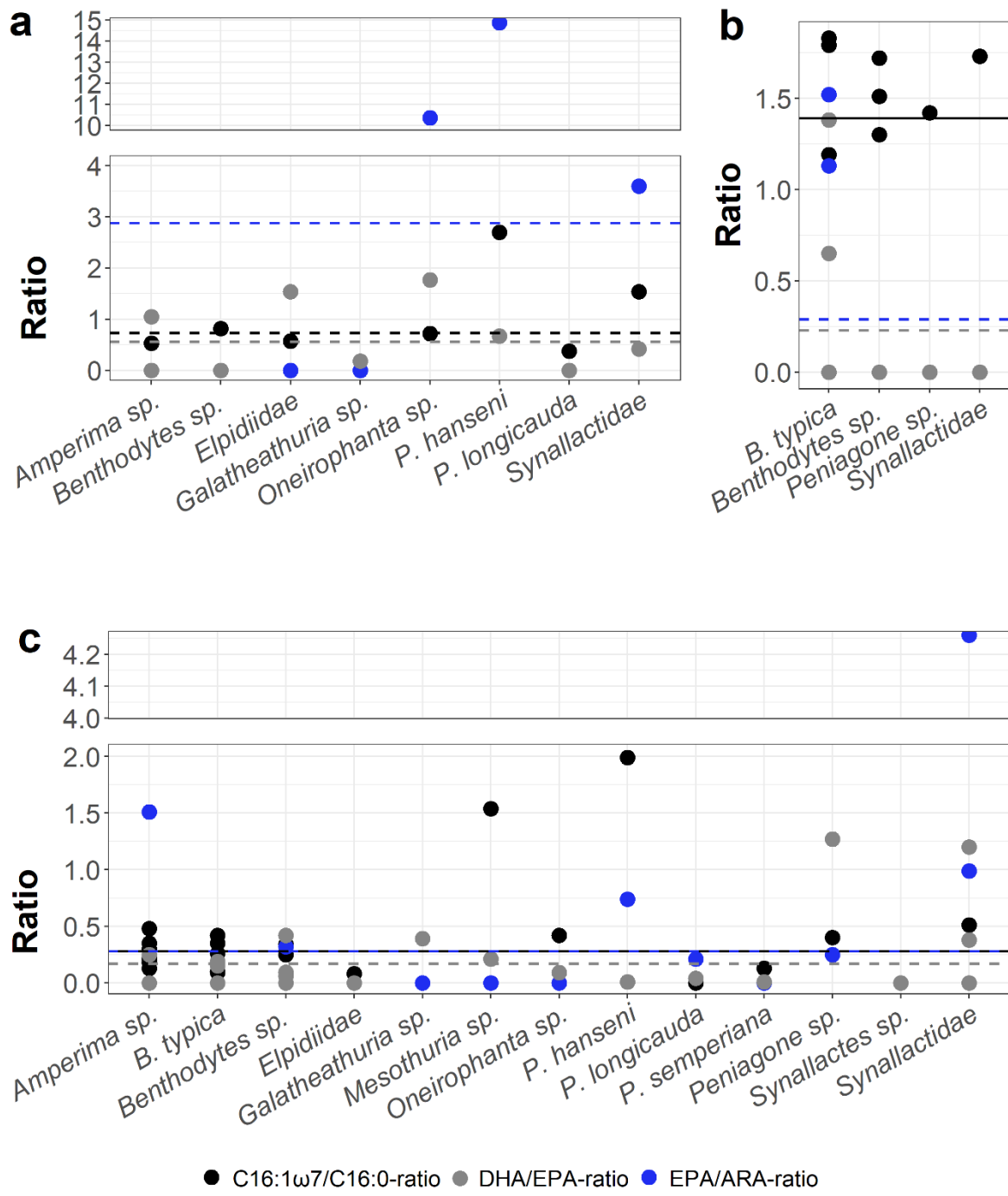
491  
492  
493

**Figure 3** continued.

494 **Table 4.** Sedimentological characteristics of holothurian gut content (GT) and feces (F). Data are presented as mean  $\pm$  1 SD and  
 495 number of replicates (n) is presented in Table S2.

| Species                                       | g dry sediment  |                 | Composition     |                 |                 |                 | Concentration factor |                 |
|---|-----------------|-----------------|-----------------|-----------------|-----------------|-----------------|----------------------|-----------------|
|   | GT              | F               | % org. C        |                 | % TN            |                 | $CF_{gut\ content}$  | $CF_{feces}$    |
|   |                 |                 | GT              | F               | GT              | F               |                      |                 |
| <b>Family: Elpidiidae</b>                     |                 |                 |                 |                 |                 |                 |                      |                 |
| <i>Amperima</i> sp.                           | 0.16 $\pm$ 0.1  | 0.54            | 7.76 $\pm$ 3.85 | 0.32            | 1.60 $\pm$ 0.71 | 0.05            | 58.0                 |                 |
| Elpidiidae gen sp.                            | 0.88            |                 | 1.57            |                 | 0.35            |                 | 14.9                 |                 |
| <i>Peniagone</i> sp.                          | 0.11            | 0.45            | 3.27            | 0.84            | 0.66            | 0.13            |                      | 4.36            |
| <b>Family: Deimatidae</b>                     |                 |                 |                 |                 |                 |                 |                      |                 |
| <i>Oneirophanta</i> sp.                       | 3.90            |                 | 2.84            |                 | 0.51            |                 | 16.6                 |                 |
| <b>Family: Laetmogonidae</b>                  |                 |                 |                 |                 |                 |                 |                      |                 |
| <i>Psychronaetes hansenii</i>                 | 12.5            |                 | 1.94            |                 | 0.38            |                 | 25.6                 |                 |
| <b>Family: Psychropotidae</b>                 |                 |                 |                 |                 |                 |                 |                      |                 |
| <i>Benthodytes</i> sp.                        | 2.07 $\pm$ 2.1  | 3.01 $\pm$ 3.61 | 0.95 $\pm$ 0.02 | 0.70 $\pm$ 0.16 | 0.16 $\pm$ 0.01 | 0.14 $\pm$ 0.05 | 1.17                 | 1.81 $\pm$ 0.53 |
| <i>Benthodytes typica</i>                     | 0.85 $\pm$ 0.62 |                 | 1.05 $\pm$ 0.47 |                 | 0.16 $\pm$ 0.01 |                 | 4.44 $\pm$ 1.52      |                 |
| <i>Psychropotes longicauda</i>                | 1.08            |                 | 1.38            |                 | 0.29            |                 | 105                  |                 |
| <i>Psychropotes semperiana</i>                | 1.78            |                 | 5.25            |                 | 0.80            |                 |                      |                 |
| <b>Family: Synallactidae</b>                  |                 |                 |                 |                 |                 |                 |                      |                 |
| <i>Synallactes</i> sp.<br>(morphotype "pink") | 6.75            |                 | 2.22            |                 | 0.34            |                 |                      |                 |
| <i>Galatheathuria</i> sp.                     | 0.51            |                 | 11.4            |                 | 2.10            |                 | 285                  |                 |
| Synallactidae gen sp.                         | 0.14            | 0.12            | 11.3            | 0.84            | 2.44            | 0.17            | 335                  |                 |

496



497 ● C16:1ω7/C16:0-ratio ● DHA/EPA-ratio ● EPA/ARA-ratio  
 498 **Figure 4.** Ratios of C16:1ω7/C16:0, DHA/EPA, and EPA/ARA in (a) holothurian gut content,  
 499 (b) holothurian feces, and (c) holothurian body wall tissue. Horizontal lines show the mean value  
 500 of a ratio based on all samples.

501 Abbreviations: ARA = arachidonic acid (C20:4ω6), DHA = docosahexaenoic acid (C22:6ω3),  
 502 EPA = eicosapentaenoic acid (C20:5ω3).

503  
 504 Feces of holothurians weighed  $1.36 \pm 2.09$  g DM feces and ranged from 0.12 g DM feces for  
 505 Synallactidae gen sp. to  $3.01 \pm 3.61$  g DM feces for *Benthodytes* sp. (Table 4). Org. C and TN

506 content of the feces was  $0.83 \pm 0.37\%$  and  $0.14 \pm 0.04\%$ , respectively, and it contained  
 507  $7.73 \pm 3.60 \mu\text{g C-PLFA g}^{-1}$  DM feces and  $7.63 \pm 5.28 \mu\text{g C-NLFA g}^{-1}$  DM feces (Fig. 3a). In  
 508 holothurian feces, PLFAs were on average still  $3.33 \pm 1.55$  times more concentrated compared to  
 509 the upper 2 cm of sediment ( $CF_{feces}$  range:  $1.81 \pm 0.53$  for *Benthodytes* sp. to  $4.44 \pm 1.52$  for *B.*  
 510 *typica*) (Table 4). The mean EPA/ARA-ratio for feces was  $0.29 \pm 0.59$ , the mean DHA/EPA-  
 511 ratio was  $0.23 \pm 0.48$ , and the mean C16:1 $\omega$ 7/C16:0-ratio was  $1.39 \pm 0.57$  (Fig. 4b).  
 512 Gut content and feces consisted of  $81.2 \pm 3.73\%$  silt (grain size:  $<63 \mu\text{m}$ ) and of  $10.7 \pm 1.10\%$   
 513 very fine sand (grain size:  $62.5 - 125 \mu\text{m}$ ) (Table 5). The median grain was  $15.5 \pm 2.27 \mu\text{m}$ .  
 514

515 **Table 5.** Grain size characteristics of gut content (GT) and feces (FC).

| Species                                     | % silt<br>fraction<br>( $<63 \mu\text{m}$ ) | % very<br>fine sand<br>fraction<br>( $62.5 - 125 \mu\text{m}$ ) | % fine<br>sand<br>fraction<br>( $125 - 250 \mu\text{m}$ ) | %<br>medium<br>sand<br>fraction<br>( $250 - 500 \mu\text{m}$ ) | % coarse<br>sand<br>fraction<br>( $500 - 1000 \mu\text{m}$ ) | Median<br>grain<br>size ( $\mu\text{m}$ ) |
|---|---|---|---|--|--|---|
| <b>Family: Elpidiidae</b>                   |   |   |   |  |  |   |
| Elpidiidae gen<br>sp. (GT)                  | 82.3  | 10.0  | 4.91  | 2.05   | 0.92   | 14.7                                      |
| <b>Family: Deimatidae</b>                   |   |   |   |  |  |   |
| <i>Oneirophanta</i><br>sp. (GT)             | 75.5  | 12.2  | 7.86  | 4.01   | 0.65   | 19.0                                      |
| <b>Family: Laetmogonidae</b>                |   |   |   |  |  |   |
| <i>Psychronaetes</i><br><i>hanseni</i> (GT) | 79.0  | 11.7  | 6.67  | 2.48   | 0.33   | 17.5                                      |
| <b>Family: Psychropotidae</b>               |   |   |   |  |  |   |
| <i>Benthodytes</i> sp.<br>(F)               | 86.4  | 9.20  | 4.05  | 0.44   | 0.00   | 13.0                                      |
| <i>Benthodytes</i><br><i>typica</i> (F)     | 81.0  | 10.8  | 6.08  | 1.77   | 0.55   | 14.2                                      |
| <b>Family: Synallactidae</b>                |   |   |   |  |  |   |
| Synallactidae<br>gen sp. (F)                | 83.0  | 10.4  | 4.47  | 1.58   | 0.76   | 14.5                                      |

516  
 517 Most of the PLFAs (Fig. 3b; Fig. S1a) and the NLFAs (Fig. 3d; Fig. S1c) found in holothurian  
 518 gut content consisted of highly unsaturated fatty acids (HUFA, i.e., fatty acids with  $\geq 4$  double  
 519 bonds;  $47.7 \pm 14.6\%$ ) and saturated fatty acids (SFA;  $40.5 \pm 11.3\%$ ), respectively, followed by  
 520 monosaturated fatty acids (MUFA), SFA, and polyunsaturated fatty acids (PUFAs, i.e., fatty  
 521 acids with  $\geq 2$  double bonds) in case of PLFAs, and followed by HUFA and MUFA in case of  
 522 NLFA.

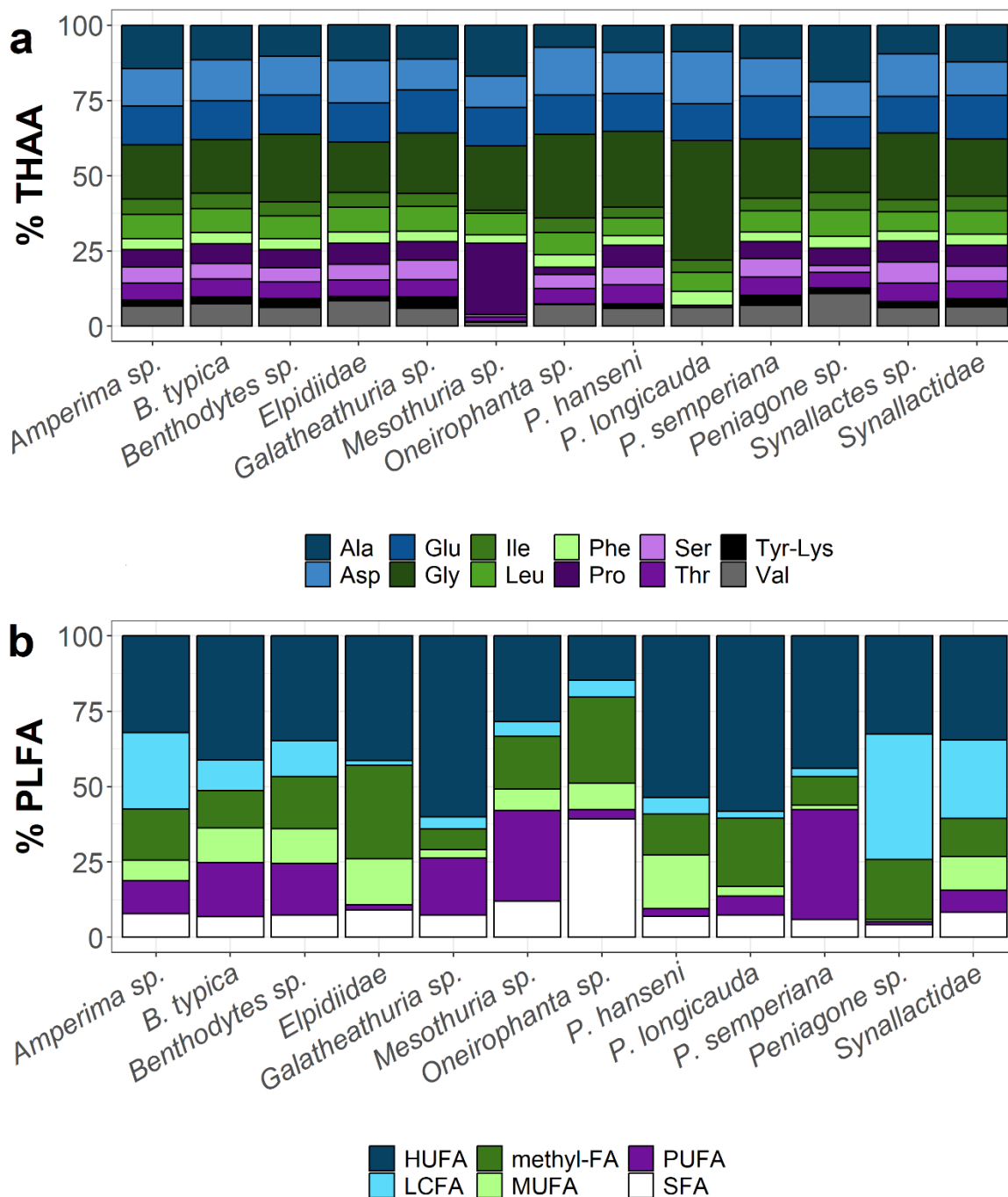
523 Feces of holothurians consisted of  $33.0 \pm 10.7\%$  PLFA-SFA (Fig. 3c; Fig. S1b) and of  
 524  $50.4 \pm 12.8\%$  NLFA-SFA (Fig. 3e; Fig. S1d). The other PLFAs consisted of  $31.7 \pm 10.5\%$   
 525 MUFA,  $16.1 \pm 11.4\%$  HUFAs, and  $10.6 \pm 23.7\%$  long-chain fatty acids (LCFA, i.e., fatty acid  
 526 with  $\geq 24$  C atoms). The NLFAs included additionally  $20.2 \pm 23.5\%$  HUFA and  $14.8 \pm 11.7\%$   
 527 MUFA.  
 528

529 **Chemical composition of holothurians**

530 Holothurians in the Peru Basin consisted of  $93.0 \pm 10.2\%$  water and their dried body walls  
531 contained  $5.08 \pm 2.89\%$  org. C and  $1.33 \pm 0.80\%$  TN, whereas their dried gut tissues consisted of  
532  $17.1 \pm 8.43\%$  org. C and  $3.76 \pm 2.18\%$  TN. The body wall and gut wall tissue of the holothurian  
533 families Deimatidae and Laetmogonidae had the highest org. C and TN contents, whereas the  
534 families Elpidiidae and Psychropotidae had the lowest org. C and TN content in body wall tissue  
535 (Table S3).

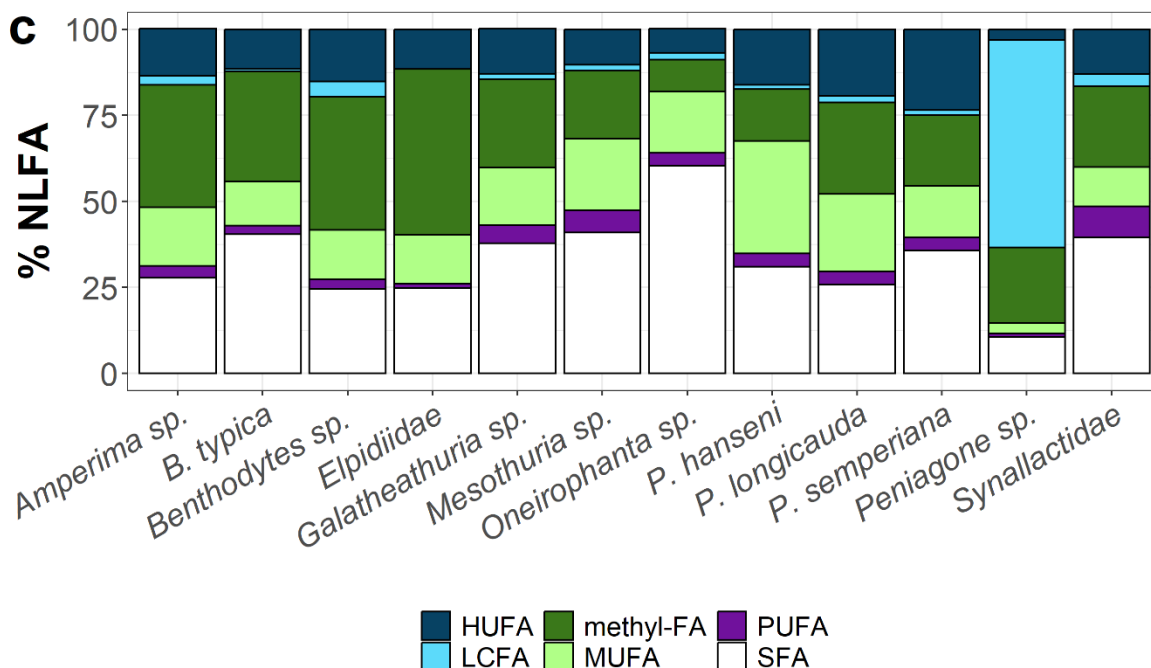
536  
537 The HAA composition did not differ greatly among species, with the main HAAs in holothurian  
538 body walls being alanine, glycine, aspartic acid, and glutamic acid, that contributed between  
539  $55.6\%$  (Elpidiidae) and  $78.2\%$  (*P. longicauda*) to total HAAs of body walls (Fig. 5a).

540



541  
 542 **Figure 5.** Contribution (%) of individual (a) hydrolysable amino acids (HAAs), (b)  
 543 phospholipid-derived fatty acid (PLFA) classes, and (c) neutral-lipid-derived fatty acid (NLFA)  
 544 classes to the total concentrations in holothurian body wall tissue.  
 545 Abbreviations of HAAs: Ala = alanine, Asp = aspartic acid, Glu = glutamic acid, Gly = glycine,  
 546 Ile = isoleucine, Leu = leucine, Met = methionine, Phe = phenylalanine, Pro = proline, Ser =  
 547 serine, Thr = threonine, Tyr-Lys = tyrosine and lysine combined, Val = valine.

548 Abbreviations of PLFA and NLFA classes: HUFA = highly unsaturated fatty acid, LCFA = long-  
 549 chain fatty acid, MUFA = monounsaturated fatty acid, PUFA = polyunsaturated fatty acid,  
 550 SFA = saturated fatty acid.  
 551



552  
 553 **Figure 5** continued.  
 554

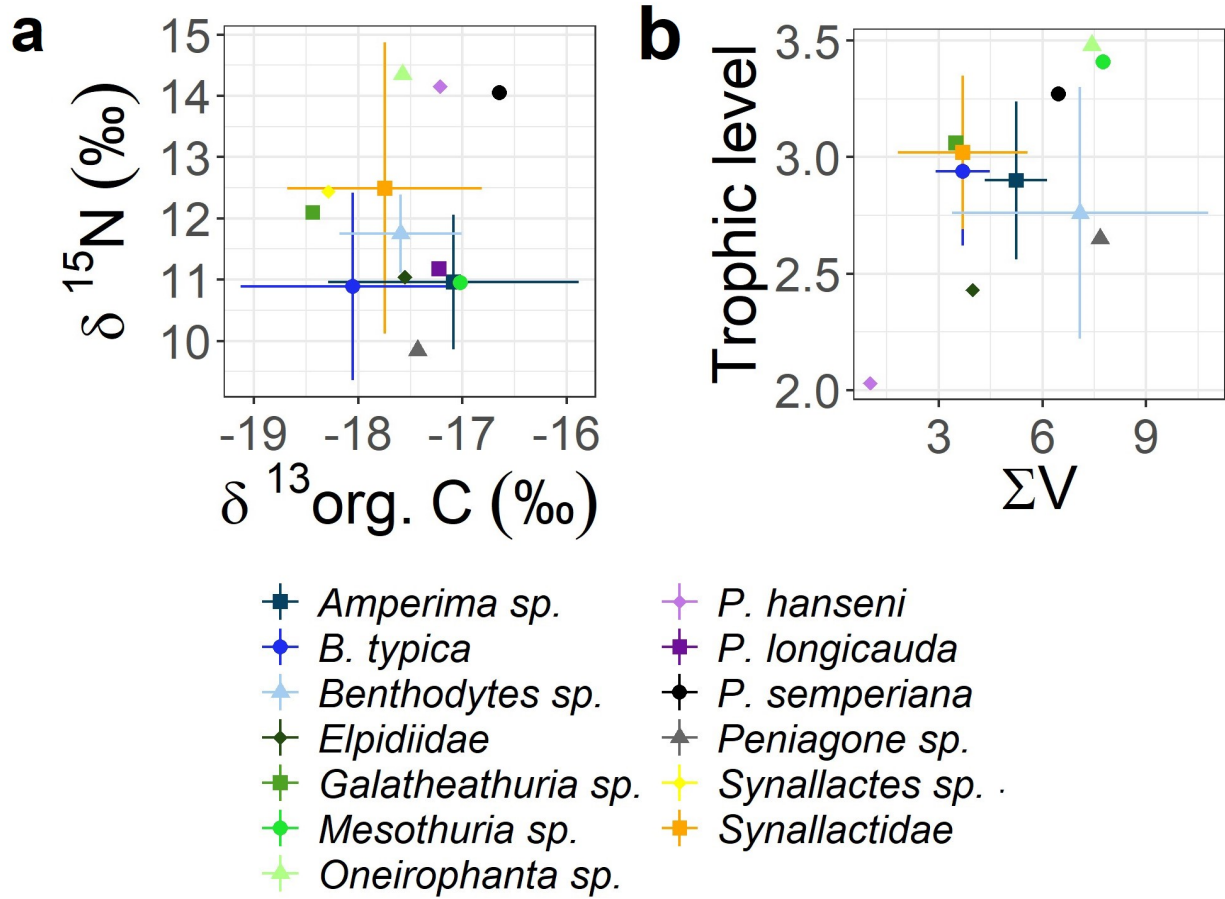
555 Across all holothurians, the metabolic amino acid threonine had a mean  $\delta^{15}\text{N}$  value of -  
 556  $9.84 \pm 8.20\text{‰}$  and source amino acids had a total mean  $\delta^{15}\text{N}$  value of  $7.49 \pm 7.81\text{‰}$  (Fig. S3).  
 557 The  $\delta^{15}\text{N}$  values of all trophic amino acids asparagine, glutamine, alanine, isoleucine, leucine,  
 558 valine, proline averaged  $20.4 \pm 4.95\text{‰}$ . The highest  $\delta^{15}\text{N}$  values for the metabolic amino acid  
 559 were measured in body wall tissue of *Amperima sp.* ( $-3.59 \pm 2.19\text{‰}$ ) and the lowest value was  
 560 measured in body wall tissue of *P. longicauda* ( $-34.4\text{‰}$ ). The highest  $\delta^{15}\text{N}$  values of source  
 561 amino acids were measured in *P. longicauda* ( $13.3 \pm 30.3\text{‰}$ ), whereas the lowest value was  
 562 found in *Oneirophanta sp.* ( $-3.75 \pm 5.05\text{‰}$ ). *P. longicauda* had the lowest  $\delta^{15}\text{N}$  values of trophic  
 563 amino acids ( $16.6 \pm 3.76\text{‰}$ ), whereas *P. semperiana* had the highest  $\delta^{15}\text{N}$  value ( $24.7 \pm 3.39\text{‰}$ ).  
 564

565 The PLFA (Fig. 5b; Fig. S2a) and NLFA (Fig. 5c; Fig. S2b) compositions differed strongly  
 566 among species. Between 1.75% (*Elpidiidae* gen sp.) and 36.6% (*P. semperiana*) of the PLFAs  
 567 found in holothurian body walls consisted of PUFAs. The other PLFA classes detected in the  
 568 body walls were HUFAs ( $36.9 \pm 13.3\%$ ), methyl-fatty acids ( $16.2 \pm 10.1\%$ ), LCFAs  
 569 ( $15.7 \pm 15.5\%$ ), MUFAs ( $9.08 \pm 12.3\%$ ), and SFAs ( $8.62 \pm 6.36\%$ ). Compared to the mean  
 570 PLFA composition across all holothurian taxa analyzed, *P. hanseni* had an above mean  
 571 percentage of MUFAs (17.7% of total PLFAs) and a below mean percentage of PUFAs (0.80%  
 572 of total PLFAs). *Oneirophanta sp.* had an above mean percentage of SFAs (39.3% of total  
 573 PLFAs) and *Galatheathuria sp.* had an above mean percentage of HUFAs (36.9% of total  
 574 PLFAs).

575 The NLFAs consisted of  $32.1 \pm 12.7\%$  SFAs, of  $15.4 \pm 6.39\%$  MUFAs, of  $3.75 \pm 2.86\%$  PUFAs,  
576 of  $13.4 \pm 6.86\%$  HUFAs, of  $4.41 \pm 11.0\%$  LCFA, and of  $31.0 \pm 16.7\%$  methyl-fatty acids. In  
577 comparison to the mean NLFA composition across all studied holothurian taxa, *Oneirophanta*  
578 sp. had an above mean percentage of SFA (60.4% of total NLFAs). *P. hanseni* had an above  
579 mean percentage of MUFAs (32.7% of total NLFAs), *P. semperiana* had an above mean  
580 percentage of HUFAs (23.5% of total NLFAs), and Elpidiidae gen sp. had an above mean  
581 percentage of methyl-fatty acids (48.1%).

582  
583 The ratio of the 'essential' phospholipid-derived PUFAs EPA to ARA, i.e., the EPA/ARA-ratio,  
584 ranged from  $0.05 \pm 0.13$  for *Benthodytes* sp. to  $1.75 \pm 2.23$  for Synallactidae gen sp. (Fig. 4c). In  
585 comparison, the ratio of DHA to EPA, i.e., the DHA/EPA-ratio, ranged from 0.01 for *P. hanseni*  
586 to 1.27 for *Peniagone* sp. (Fig. 4c). Due to the absence of the PUFAs ARA and/ or EPA in  
587 holothurian body wall tissue, no EPA/ARA-ratios were calculated for *B. typica*, Elpidiidae gen  
588 sp., *Galatheathuria* sp., *Mesothuria* sp., *Oneirophanta* sp., and *P. semperiana*. Elpidiidae gen sp.  
589 lacked both, DHA and EPA, and therefore no DHA/EPA-ratio could be calculated (Fig. 4c).

590  
591 **Trophic position of holothurians and recycling of amino acids**  
592 Holothurians in the Peru Basin had a mean  $\delta^{13}\text{C}$ -value of  $-17.5 \pm 0.89\text{‰}$  with a minimum  
593 value of  $-16.6\text{‰}$  for *P. semperiana* and a maximum value of  $-18.4\text{‰}$  for *Galatheathuria* sp. The  
594 mean  $\delta^{15}\text{N}$ -value was  $11.6 \pm 1.47\text{‰}$  with a minimum value of  $9.84\text{‰}$  for *Peniagone* sp. and a  
595 maximum value of  $14.3\text{‰}$  for *Oneirophanta* sp. (Fig. 6a).  
596 Trophic level (TL) estimates for holothurians in the Peru Basin, based on the  $\delta^{15}\text{N}$  values of the  
597 HAA glutamic acid and alanine, ranged from 2.0 (*P. hanseni*;  $\sigma_{TL}$ :  $\pm 0.44$ ) to 3.5 (*Oneirophanta*  
598 sp.;  $\sigma_{TL}$ :  $\pm 0.44$ ) (Fig. 6b).  
599  $\Sigma V$  values ranged from 1.02 to 7.76, with *P. hanseni* having the lowest heterotrophic enrichment  
600 and *Mesothuria* sp. having the highest heterotrophic enrichment (Fig. 6b).  
601

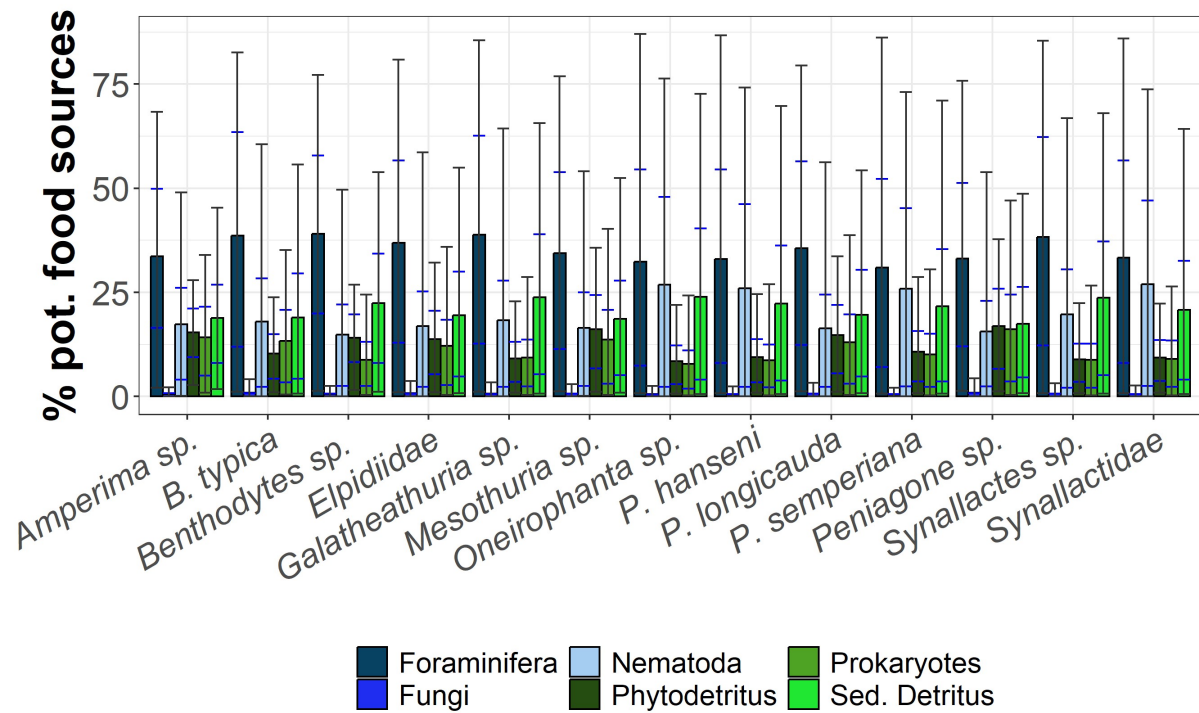


602 **Figure 6.** (a) Isotopic composition of carbon ( $\delta^{13}\text{org. C}$ , ‰) and N ( $\delta^{15}\text{N}$ , ‰) of holothurian  
 603 body wall tissue from the Peru Basin. (b) Trophic level (TL) and heterotrophic enrichment factor  
 604  $\Sigma V$  of holothurians. Error bars in indicate 1 SD.

606 **Mixing model results (MixSIAR)**

607 Bayesian mixing model results suggested that potential food sources of holothurians in the Peru  
 608 Basin were (in order) Foraminifera, sedimentary detritus, Nematoda, phytodetritus, prokaryotes,  
 609 and Fungi (<0.1%) (Fig. 7).

611



612  
 613 **Figure 7.** Results of SIAR Bayesian mixing model showing the mean contribution of each  
 614 potential food source (%) to the diet of the different holothurian species in the Peru Basin. Error  
 615 bars in blue indicate 25% and 75% Bayesian credibility intervals (BCI), and error bars in gray  
 616 present 5% and 95% BCI.

617  
 618 The contribution of Foraminifera ranged from  $31.0 \pm 28.2\%$  (5 – 95% Bayesian credibility  
 619 intervals BCI: 0.70 – 86.2%) to  $39.1 \pm 23.6\%$  (5 – 95% BCI: 1.30 – 77.2%) and  $38.6 \pm 27.7\%$  (5  
 620 – 95% BCI: 1.10 – 82.6%) to the total food sources of *P. semperiana*, *Benthodytes* sp., and *B.*  
 621 *typica*, respectively, whereas sedimentary detritus potentially contributed between  $17.5 \pm 15.8\%$   
 622 (5 – 95% BCI: 0.80 – 48.7%) and  $23.8 \pm 21.5\%$  (5 – 95% BCI: 0.70 – 65.6%) to the total diet of  
 623 *Peniagone* sp. and *Galatheathuria* sp. Phytodetritus was suggested to account for  $8.50 \pm 6.80\%$   
 624 (5 – 95% BCI: 0.70 – 22.0%) to  $16.9 \pm 11.8\%$  (5 – 95% BCI: 1.20 – 37.8%) to the food sources  
 625 of *Oneirophanta* sp. and *Peniagone* sp., and heterotrophic prokaryotes contributed between  
 626  $7.80 \pm 16.1\%$  (5 – 95% BCI: 0.30 – 24.3%) and  $16.1 \pm 15.5\%$  (5 – 95% BCI: 0.40 – 47.1%) to  
 627 the diets of the same species. However, the large 25%/ 75% and 5%/ 95% BCI ranges (Fig. 7)  
 628 indicate that the capacity of the models to resolve the contributions of potential food sources was  
 629 low, likely due to the implementation of published stable isotopic composition data that were  
 630 mostly not site-specific. Hence, the model outcomes should be interpreted with care.

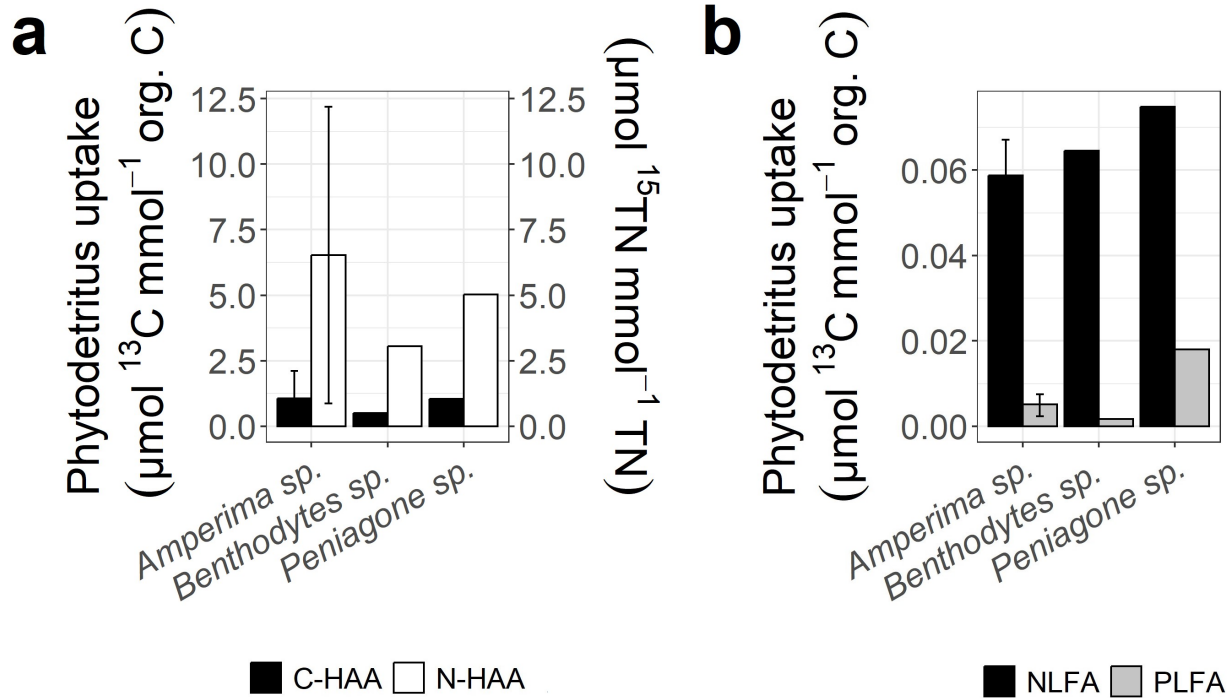
631  
 632 **Fresh phytodetritus uptake by holothurians**

633 Within three days, the holothurians in the feeding experiment took up  $0.021 \pm 0.014$  mmol  
 634 phytodetritus C  $\text{mmol}^{-1}$  org. C (*Amperima* sp.:  $0.017 \pm 0.014$ ; *Peniagone* sp.:  $0.039$ ; *Benthodytes*  
 635 sp.:  $0.018$ ) and  $0.017 \pm 0.013$  mmol phytodetritus N  $\text{mmol}^{-1}$  TN (*Amperima* sp.:  $0.013 \pm 0.012$ ;  
 636 *Peniagone* sp.:  $0.036$ ; *Benthodytes* sp.:  $0.016$ ). Gut content of holothurians collected after three  
 637 days still contained  $0.122 \pm 0.223$  mmol phytodetritus C  $\text{g}^{-1}$  DM gut content and  
 638  $0.083 \pm 0.164$  mmol phytodetritus N  $\text{g}^{-1}$  DM gut content. The feces of 1 *Amperima* sp. specimen

639 even included 0.036 mmol phytodetritus C g<sup>-1</sup> DM feces and 0.028 mmol phytodetritus N g<sup>-1</sup>  
 640 DM feces.

641  
 642 Holothurians incorporated 0.95 ± 0.78 μmol <sup>13</sup>C-HAA mmol<sup>-1</sup> org. C (min: 0.51, *Benthodytes*  
 643 sp.; max: 1.06 ± 1.05, *Amperima* sp.) and 5.53 ± 4.28 μmol <sup>15</sup>N-HAA mmol<sup>-1</sup> TN (min: 3.05,  
 644 *Benthodytes* sp.; 6.53 ± 5.66, *Amperima* sp.) (Fig. 8a).

645

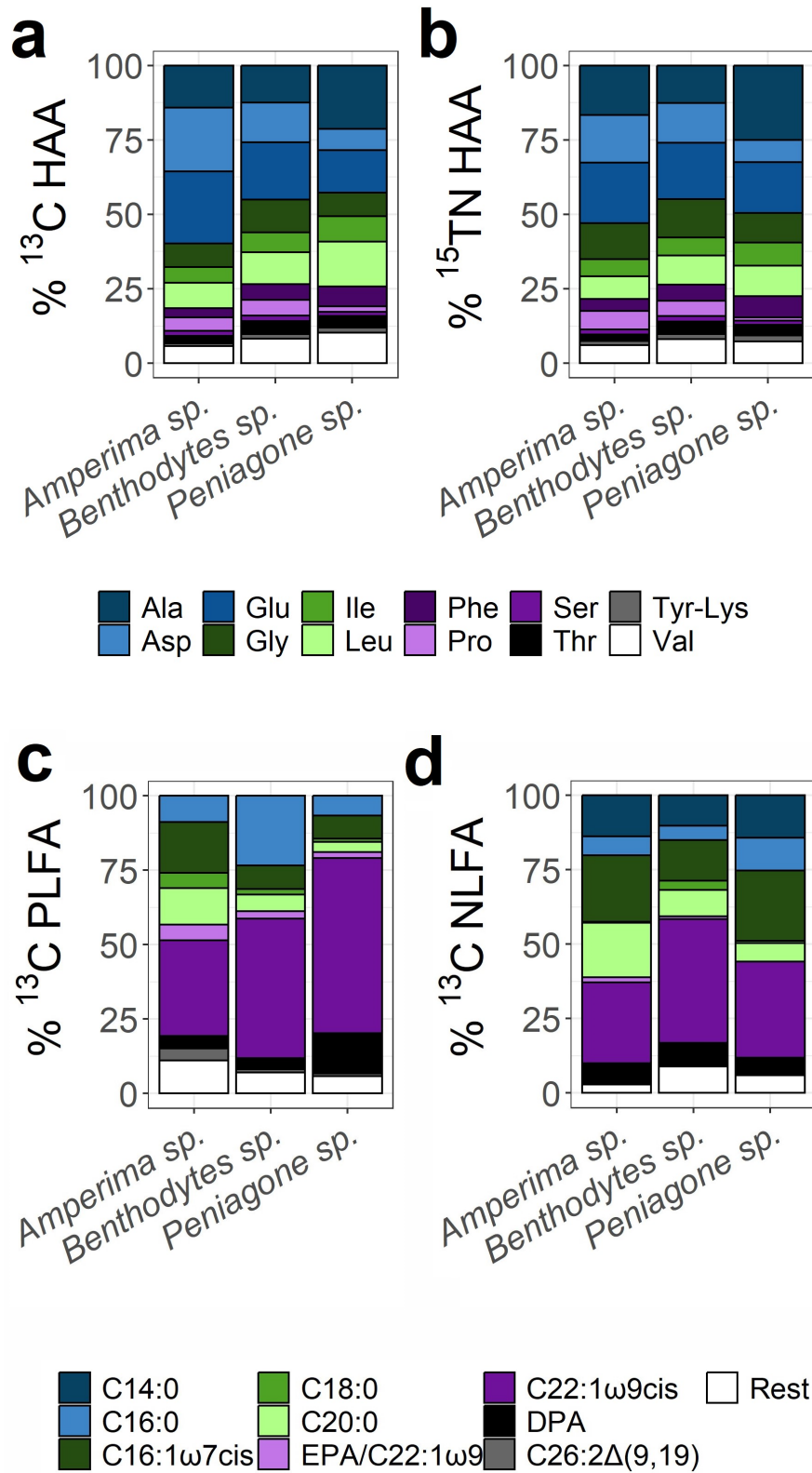


646  
 647 **Figure 8.** Uptake of phytodetritus C and N in the compounds (a) HAAs (μmol <sup>13</sup>C mmol<sup>-1</sup> org.  
 648 C, μmol <sup>15</sup>N mmol<sup>-1</sup> TN), (b) PLFAs (μmol <sup>13</sup>C mmol<sup>-1</sup> org. C) and NLFAs (μmol <sup>13</sup>C mmol<sup>-1</sup>  
 649 org. C) of holothurian tissue from the *in-situ* experiment.  
 650 Error bars indicate 1 SD.

651  
 652 Most of the <sup>13</sup>C in HAAs consisted of <sup>13</sup>C in glutamic acid (21.3 ± 8.93 %), in aspartic acid  
 653 (16.9 ± 11.1%), and in alanine (15.3 ± 4.86%) (Fig. 9a), whereas most of the <sup>15</sup>N in HAAs was  
 654 incorporated in the amino acids glutamic acid (19.5 ± 1.46%), alanine (17.5 ± 5.25%), and  
 655 aspartic acid (13.7 ± 4.91%) (Fig. 9b).

656 Holothurians incorporated 0.007 ± 0.007 μmol <sup>13</sup>C-PLFA mmol<sup>-1</sup> org. C (min: 0.002,  
 657 *Benthodytes* sp., max: 0.018, *Peniagone* sp.) and 0.064 ± 0.030 μmol <sup>13</sup>C-NLFA mmol<sup>-1</sup> org. C  
 658 (min: 0.059 ± 0.050, *Amperima* sp., max: 0.075, *Peniagone* sp.) (Fig. 8b). Most of the <sup>13</sup>C in  
 659 PLFAs consisted of <sup>13</sup>C in C22:1ω9 *cis* (40.3 ± 23.1%), in C16:1ω7 *cis* (13.4 ± 7.33%), and in  
 660 C16:0 (11.4 ± 7.53%) (Fig. 9c), whereas most of the <sup>13</sup>C in NLFAs was incorporated in  
 661 C22:1ω9 *cis* (32.1 ± 23.2%), C16:1ω7 *cis* (20.5 ± 9.16%), C20:0 (12.9 ± 8.49%), and C14:0  
 662 (13.0 ± 3.30%) (Fig. 9d).

663



664  
665  
666  
667

**Figure 9.** Contribution (%) of individual (a) phytodetritus C and (b) N uptake in hydrolysable amino acids (HAAs) to total phytodetritus C and N uptake in HAA and (c, d) contribution (%) of phytodetritus C uptake by individual phospholipid-derived fatty acids (PLFAs) and neutral-lipid-

668 derived fatty acids (NLFAs) to total phytodetritus C uptake in PLFAs and NLFAs of holothurian  
669 body wall tissue from the *in-situ* experiment. The PLFA and NLFA pools 'Rest' include all  
670 PLFAs and NLFAs, respectively, that contribute <2.5% to total % phytodetritus C uptake in  
671 PLFA or NLFA of the mean holothurian body wall tissue from the *in-situ* experiment.  
672 Abbreviations of HAAs: Ala = alanine, Asp = aspartic acid, Glu = glutamic acid, Gly = glycine,  
673 Ile = isoleucine, Leu = leucine, Met = methionine, Phe = phenylalanine, Pro = proline, Ser =  
674 serine, Thr = threonine, Tyr-Lys = tyrosine and lysine combined, Val = valine.  
675 Abbreviations of PLFAs and NLFAs: DPA = docosapentaenoic acid (C22:5 $\omega$ 3), EPA =  
676 eicosapentaenoic acid (C20:5 $\omega$ 3).

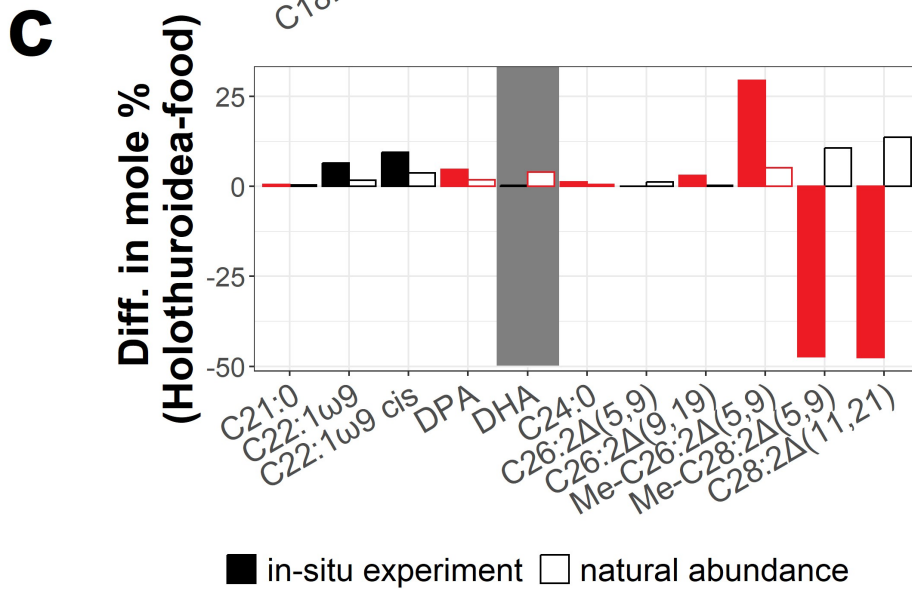
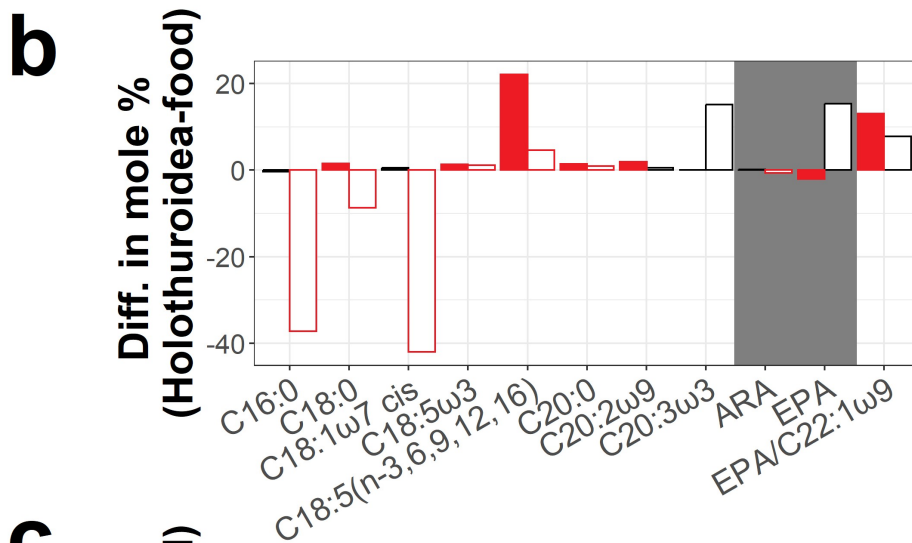
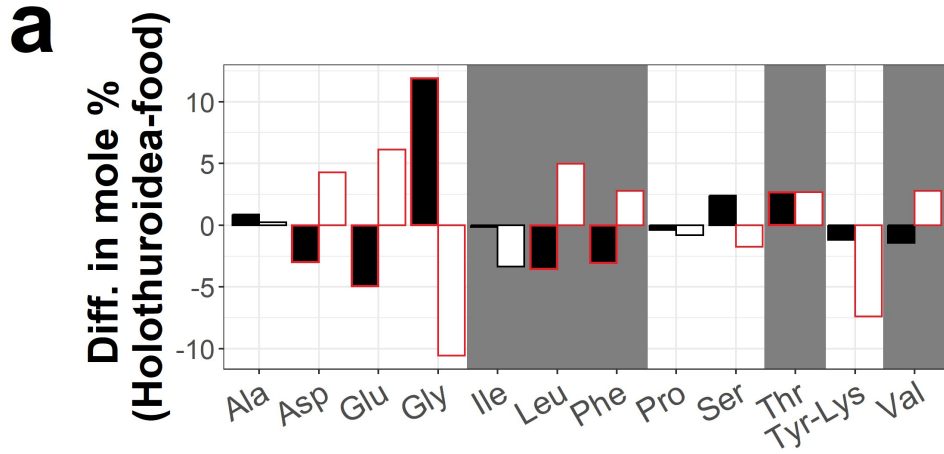
677

### 678 **Dependence of holothurians on sediments and fresh phytodetritus**

679 The HAAs aspartic acid, glutamic acid, leucine, phenylalanine, threonine, and valine occurred in  
680 statistically higher proportions in holothurians from the Peru Basin than in the surface sediment  
681 (0 – 2 cm) (Wilcoxon rank sum tests  $W$ ,  $p \leq 0.05$ ; Table S4, Fig. 10a), implying a net  
682 accumulation of these amino acids. In comparison, the amino acids glycine, serine, and tyrosine  
683 and lysine combined showed a net deficiency, i.e., their proportions were statistically  
684 significantly higher in the surface sediment compared to the tissue of holothurians (Wilcoxon  
685 rank sum tests  $W$ ,  $p \leq 0.05$ ; Table S4, Fig. 10a).

686 In the *in-situ* experiment, the difference in mole percentages of amino acids indicated a net  
687 deficiency of holothurians in aspartic acid, glutamic acid, leucine, phenylalanine (Wilcoxon rank  
688 sum tests  $W$ ,  $p \leq 0.05$ ; Table S4, Fig. 10a). In comparison, holothurians from this experiment had  
689 a net accumulation of glycine and threonine compared to the phytodetritus (Wilcoxon rank sum  
690 tests  $W$ ,  $p \leq 0.05$ ; Table S4, Fig. 10a).

691



692  
693  
694

**Figure 10.** Comparison of the mean difference in mole percentages (a) of hydrolysable amino acids (HAAs) and (b, c) phospholipid-derived fatty acids (PLFAs) between holothurian body

695 wall tissue and the corresponding food source (natural abundance *in-situ* experiment  
696 holothurians with the 0 – 2 cm sediment layer, white bars; Holothurians from the *in-situ*  
697 experiment with <sup>13</sup>C- and <sup>15</sup>N-enriched phytodetritus, black bars). The grey shading highlights  
698 ‘essential’ amino acids (Phillips 1984) and fatty acids (Glencross 2009). Statistical differences in  
699 mole percentages between were determined by Wilcoxon rank sum tests (Table S4) and  
700 indicated by the red outlines.

701 Abbreviations of HAAs: Ala = alanine, Asp = aspartic acid, Glu = glutamic acid, Gly = glycine,  
702 Ile = isoleucine, Leu = leucine, Met = methionine, Phe = phenylalanine, Pro = proline, Ser =  
703 serine, Thr = threonine, Tyr-Lys = tyrosine and lysine combined, Val = valine.

704 Abbreviations of PLFAs and NLFAs: ARA = arachidonic acid (C20:4 $\omega$ 6), DHA =  
705 docosahexaenoic acid (C22:6 $\omega$ 3), DPA = docosapentaenoic acid (C22:5 $\omega$ 3), EPA =  
706 eicosapentaenoic acid (C20:5 $\omega$ 3).

708 An assessment of PLFAs that contributed on average  $\geq 1\%$  to total PLFAs in body wall tissue of  
709 holothurians from the Peru Basin showed that the PLFAs C18:5 $\omega$ 3, C18:5(n-3,6,9,12,16), C20:0,  
710 docosapentaenoic acid (DPA, C22:5 $\omega$ 3), DHA, C24:0, and Me-C26:2 $\Delta$ (5,9) were present in  
711 statistically higher proportions in holothurians than in surface sediment (0 – 2 cm) (Wilcoxon  
712 rank sum tests *W*,  $p \leq 0.05$ ; Table S4, Fig. 10b, c), indicating a net accumulation of these PLFAs  
713 in holothurian tissue. The PLFAs C16:0, C18:0, C18:1 $\omega$ 7 *cis*, and ARA had net deficiencies in  
714 holothurians (Wilcoxon rank sum tests *W*,  $p \leq 0.05$ ; Table S4, Fig. 10b, c).

715 In the *in-situ* experiment, the difference in mole percentages of PLFA ( $\geq 1\%$  of total PLFAs in  
716 body-wall tissue in *in-situ* holothurians) pointed towards a net accumulation of C18:0, C18:5 $\omega$ 3,  
717 C18:5(n-3,6,9,12,16), C20:0, C20:2 $\omega$ 9, EPA/C22:1 $\omega$ 9, C21:0, DPA, C24:0, C26:2 $\Delta$ (9,19), and  
718 Me-C26:2 $\Delta$ (5,9) in holothurian tissue (Wilcoxon rank sum tests *W*,  $p \leq 0.05$ ; Table S4, Fig. 10b,  
719 c). In comparison, holothurians had a net deficiency of EPA, Me-C28:2 $\Delta$ (5,9), and  
720 C28:2 $\Delta$ (11,21) (Wilcoxon rank sum test *W*,  $p < 0.04$ ; Table S4, Fig. 10b, c) compared to the  
721 phytodetritus.

722

## 723 Discussion

724 For most of the holothurian species present in the Peru Basin, very little to no information is  
725 available about their feeding strategies and diet preferences. Therefore, we first infer feeding  
726 strategies for holothurians based on CSIA and subsequently we explore whether resource  
727 partitioning exists that could facilitate the high holothurian biodiversity in the Peru Basin.  
728 Finally, we discuss how holothurians affect organic C availability in sediments of the Peru Basin,  
729 and whether holothurians are dependent on amino acids and phospholipid-derived fatty acids  
730 from fresh phytodetritus.

731

### 732 Holothurians trophic level and inferred feeding strategy

733 Based on the  $\delta^{15}\text{N}$  value of body wall tissue, Iken et al., (2001) identified three trophic groups  
734 among holothurians from PAP: Group A had  $\delta^{15}\text{N}$  values from 10.8 to 12.3‰, group B’s  $\delta^{15}\text{N}$   
735 values ranged from 13.2 to 13.9‰, and group C had  $\delta^{15}\text{N}$  values from 15.6 to 16.2‰. The  $\delta^{15}\text{N}$   
736 values of holothurian tissue from the Peru Basin investigated in this study were lower and ranged  
737 from 9.84‰ for *Peniagone* sp. to 14.4‰ for *Oneirophanta* sp. Instead of basing our  
738 classification of holothurians from the Peru Basin solely on  $\delta^{15}\text{N}$  values, we combined data of  
739 trophic level based on CSIA (amino acids, fatty acids) with results of a Bayesian mixing model,  
740 biomarkers, grain size analysis, and concentration factors for PLFAs.

741  
742 CSIA of amino acids allows to calculate the total heterotrophic re-synthesis of amino acids  $\sum V$   
743 which is a proxy for “heterotrophic reworking of proteinaceous material” (McCarthy et al. 2007).  
744 In the context of holothurians,  $\sum V_{body-wall\ tissue} > \sum V_{sediment}$  indicates that the heterotrophic  
745 gut microbiome re-works detritus that was ingested by the holothurians or that holothurians  
746 selectively consume material that has undergone more re-working. Among various holothurian  
747 species, species with a low  $\sum V$  value likely ingest more phytodetritus than sedimentary detritus  
748 compared to species with a high  $\sum V$  value, as McCarthy et al. (2007) detected a linear increase  
749 in  $\sum V$  from algae, via zooplankton, to detrital material.  
750 When deep-sea holothurians have source amino acids in their gut contents that are enriched in  
751  $^{15}\text{N}$  relative to sediments, these holothurians are likely secondary consumers of detritus, whereas  
752 the microbial community in their guts are primary consumers of detritus (Romero-Romero et al.  
753 2021).

754  
755 Ratios of the fatty acids C16:1 $\omega$ 7 to C16:0 and DHA to EPA are biomarkers for diatoms when  
756  $\frac{C16:1\omega7}{C16:0} > 1$  or  $\frac{DHA}{EPA} < 1$  (Kharlamenko et al. 1995; Budge and Parrish 1998; Dalsgaard et al. 2003;  
757 Parrish et al. 2005) and for dinoflagellates when  $\frac{C16:1\omega7}{C16:0} < 1$  or  $\frac{DHA}{EPA} > 1$  (Budge and Parrish 1998;  
758 Dalsgaard et al. 2003; Parrish et al. 2005).

#### 759 760 **Order Elasipodida**

761 *P. hanseni* (n = 1) is a deposit feeder of the **family Laetmogonidae**, which has a trophic level of  
762 2.0, a low level of heterotrophic re-synthesis of amino acids and feeds selectively on sedimentary  
763 detritus particles of a medium grain size of 17.5  $\mu\text{m}$  which is smaller than the medium grain size  
764 of the upper 5 cm of sediment ( $20.8 \pm 0.3 \mu\text{m}$ ; Mevenkamp et al., 2019). Based on the  
765 biomarkers present in the body wall tissue of the specimen analyzed and in its gut content,  
766 (large) parts of the sedimentary detritus likely consist of diatom-derived phytodetritus.

767  
768 Elpidiidae gen sp. (n = 1) (**family Elpidiidae**) has a trophic level of 2.4 and medium level of  
769 heterotrophic re-synthesis of amino acids. This species is a selective deposit feeder that might  
770 ingest sedimentary detritus (Bayesian mixing model:  $19.5 \pm 17.6\%$  contribution; 5% – 95% BCI:  
771 0.80% – 54.9%) and/ or Foraminifera (Bayesian mixing model:  $36.9 \pm 25.9\%$  contribution; 5% –  
772 95% BCI: 1.00% – 80.9%). Though, this result should be interpreted with caution due to the low  
773 capability of the Bayesian mixing model to constrain the contribution of the potential food  
774 sources.

775  
776 The benthopelagic *Peniagone* sp. (n = 1) of the **family Elpidiidae** has an estimated trophic level  
777 of 2.7 and a very high level of heterotrophic re-synthesis of amino acids. This species has a  
778 ‘sweeping’ feeding style (Roberts et al. 2000) and was found to assimilate fresh phytodetritus at  
779 PAP (Iken et al. 2001) with medium efficiency, as the PLFA concentration in its feces ( $CF_{feces}$ ) is  
780 four times higher than in the surface sediment (this study). In the Peru Basin, *Peniagone* sp.  
781 seems to feed on diatom-derived phytodetritus, but likely also on sedimentary detritus as  
782 indicated by the high  $\sum V$  value. In fact, the poorly resolved Bayesian mixing model suggests an  
783 equal contribution of phytodetritus ( $16.9 \pm 11.8\%$ ; 5% – 95% BCI: 1.20% – 37.8%) and  
784 sedimentary detritus ( $17.5 \pm 15.8\%$ ; 5% – 95% BCI: 0.80% – 48.7%) to the holothurian diet.

785

786 *Amperima* sp. (n = 9) belongs to the **family Elpidiidae** and its trophic level was estimated to be  
787  $2.9 \pm 0.3$ , potentially due to a medium level of heterotrophic re-synthesis of amino acids. This  
788 species is a very selective surface deposit feeder with a ‘sweeping’ feeding style (Roberts et al.  
789 2000) that grazes on very fresh phytodetritus on the surface sediment (Iken et al. 2001). As a  
790 result, the gut content of *A. rosea* at PAP has higher concentrations of chlorophyll-*a* compared to  
791 surface sediment or phytodetritus (FitzGeorge-Balfour et al. 2010). A more detailed analysis of  
792 the phytopigments in this gut content revealed that *A. rosea* at PAP feeds preferentially on  
793 cyanobacteria-derived phytodetritus (Wigham et al. 2003a). Based on the PLFA composition of  
794 its gut content, we found that *Amperima* sp. from the Peru Basin likely feeds on dinoflagellate-  
795 derived phytodetritus. Also, the body wall fatty acid composition in our study differs  
796 substantially from specimens from PAP, as the PLFA profile of PAP specimens is dominated by  
797 EPA, DHA, ARA, and C18:0 (Hudson et al. 2004), whereas the PLFA profile of Peru Basin  
798 specimens is characterized mostly by EPA co-eluted with C22:1 $\omega$ 9, Me-C26:2 $\Delta$ (5,9), and  
799 C28:2 $\Delta$ (11,21). Hence, it seems that the diet preferences of the well-studied *Amperima* sp. can  
800 differ substantially between ocean basins.

801  
802 *Benthodytes* sp. (n = 6) from the **family Psychropotidae** has an estimated trophic level of  
803  $2.8 \pm 0.5$  and a very high level of heterotrophic re-synthesis of amino acids. It feeds with a  
804 ‘sweeper’ feeding style (Roberts et al. 2000) selectively on smaller sediment particles (medium  
805 grain size: 13.0  $\mu$ m) from the surface sediment. However, it likely does not or only moderately  
806 selects for specifically detritus-enriched particles. In fact, the high percentage of the bacteria-  
807 biomarker PLFAs C16:0, C16:1 $\omega$ 7 *cis*, and C18:1 $\omega$ 7 *cis* in its gut content and feces and the very  
808 high level of heterotrophic re-synthesis of amino acids indicates *Benthodytes* sp. hosts a large  
809 biomass of living heterotrophic prokaryotes. Though, the mean  $\delta^{15}\text{N}_{\text{source AA}}$ -value is below the  
810 mean  $\delta^{15}\text{N}_{\text{source AA}}$ -value across all holothurians investigated in this study, we hypothesize that  
811 *Benthodytes* sp. is a secondary consumer, and its microbial gut community is the primary  
812 consumer of detritus.

813  
814 *B. typica* (n = 5) belongs to the **family Psychropotidae** and its trophic level is comparable (2.9)  
815 to the trophic level of *Benthodytes* sp. This species has a medium level of heterotrophic re-  
816 synthesis of amino acids and feeds selectively on smaller particles (medium grain size: 14.2  $\mu$ m)  
817 from the ambient sediment. These smaller particles contain a four times higher PLFA  
818 concentration than the surrounding sediment and consist partially of diatom-derived  
819 phytodetritus. Reliance on phytodetritus is confirmed by the PLFA composition of *B. typica*  
820 body walls. In addition, this species either feeds selectively on sediment-bound prokaryotes or  
821 hosts prokaryotes because bacteria-specific PLFAs (i.e., C16:0, C16:1 $\omega$ 7 *cis*, and C18:1 $\omega$ 7 *cis*)  
822 contribute almost 30% to the total PLFA composition in feces. Also, the mean  $\delta^{15}\text{N}_{\text{source AA}}$ -value  
823 is enriched compared to the mean  $\delta^{15}\text{N}_{\text{source AA}}$ -value across all holothurians. Since a medium  
824 level of heterotrophic re-synthesis of amino acids was measured, *B. typica* likely has a mixed  
825 diet: In this diet, this holothurian species consumes phytodetritus as primary consumer and other  
826 types of detritus as secondary consumer following primary processing by the gut microbiome.

827  
828 *P. longicauda* (n = 1) from the **family Psychropotidae** has a medium level of heterotrophic re-  
829 synthesis of amino acids. Feeding selectivity was the highest in our data, though, surprisingly, at  
830 PAP this species was found to feed less selectively than *P. diaphana* (FitzGeorge-Balfour et al.  
831 2010). *P. longicauda*’s diet consists likely mainly of diatom-derived phytodetritus, but it is also

832 possible that *P. longicauda* consumes filamentous Rhodophyceae. This algae has been found in  
833 gelatinous detritus in the deep sea of the NE Atlantic and Bühring et al., (2002) speculated that  
834 *P. longicauda* might feed on it sporadically, because the body walls of *P. longicauda* from  
835 specimens collected at PAP and in the Peru Basin contain EPA, a PLFA typical for  
836 Rhodophyceae, at relatively high concentrations (31% of total PLFA, this study; ~24% of total  
837 fatty acids at PAP; Ginger et al. 2000). Additionally, at PAP 70 to 80% of the gut content of this  
838 species contained sediment (Iken et al. 2001), which might originate from foraminiferans that  
839 Roberts and Moore, (1997) found in its guts together with radiolarians, harpacticoids, nematodes,  
840 spicules, and diatoms.

841  
842 *P. semperiana* (n = 1) (**family Psychropotidae**) has an estimated trophic level of 3.3, likely  
843 related to the high level of heterotrophic re-synthesis of amino acids. This species has been  
844 classified as surface deposit feeder (Iken et al. 2001) and based on the biomarkers in the body  
845 tissue of a specimen collected in the Peru Basin, it might also consume diatom-derived  
846 phytodetritus.

#### 847 **Order Holothuriida**

848  
849 *Mesothuria* sp. (n = 1) belongs to the **family Mesothuriidae** and has an estimated trophic level  
850 of 3.4. This species could be a subsurface (Iken et al. 2001) or surface deposit feeder (Miller et  
851 al. 2000) with a ‘raker’ feeding style (Roberts et al. 2000) or feeding with a ‘wiping’ motion  
852 (Hudson et al. 2005). The PLFA composition of its body walls suggests that *Mesothuria* sp.  
853 likely consumes diatom-derived phytodetritus. Indeed, in a study on the Hawaiian slope, gut  
854 contents of *Mesothuria carnosa* Fisher, 1907, had a 2.7-fold enrichment of chlorophyll-a  
855 pointing towards selective feeding on phytodetritus (Miller et al. 2000). Furthermore, the very  
856 high level of heterotrophic re-synthesis of amino acids from the Peru Basin suggests that  
857 *Mesothuria* sp. might also be a secondary consumer of detritus. However, we lack information  
858 about its gut content to confirm that it hosts a big(ger) living microbial biomass in its gut that is  
859 the primary consumer of detritus.

#### 860 **Order Synallactida**

861  
862 *Oneirophanta* sp. (n = 1) as member of the **family Deimatidae** has an estimated trophic level of  
863 3.5 and a very high level of heterotrophic re-synthesis of amino acids. This species feeds  
864 selectively with a ‘raker’ feeding style (Roberts et al. 2000) and takes up particles with a median  
865 grain size of 19.0 µm, which is slightly smaller than the median grain size of sediment particles  
866 in the Peru Basin (Mevenkamp et al. 2019). The specimen collected in the Peru Basin likely fed  
867 on diatom-derived phytodetritus and maybe on bacteria. The very high level of heterotrophic re-  
868 synthesis of amino acids and the high trophic level of *Oneirophanta* sp. points to the role of a  
869 secondary consumer of detritus, whereby a big biomass of microbial gut community serves as  
870 first consumers. However, bacteria specific PLFAs C16:0, C16:1ω7 cis, and C18:1ω7 cis, that  
871 were detected in high concentrations in the gut content of *Benthodytes* sp., contribute only 5% to  
872 the total PLFA composition in the gut content of *Oneirophanta* sp. Therefore, the diet  
873 preferences of this species in the Peru Basin are less clear.

874  
875 Synallactidae gen sp. (n = 3) (**family Synallactidae**) has an estimated trophic level of  $3.0 \pm 1.5$   
876 and a medium level of heterotrophic re-synthesis of amino acids. It feeds extremely selectively  
877 and consumes particles of a median grain size that is smaller than the median grain size of the

878 surface sediment in the Peru Basin. The PLFA composition of the body wall and the gut content  
879 of Synallactidae gen sp. indicates that this species predates upon agglutinated foraminiferans,  
880 and it consumes diatom-derived phytodetritus. However, it is not possible to differentiate  
881 whether Synallactidae gen sp. is a primary consumer of the phytodetritus or a secondary  
882 consumer, whereupon the foraminiferans are the primary consumer. The PLFA composition of  
883 the feces shows that this holothurian species is also a bacterivore as bacteria specific PLFAs (i.e.,  
884 C16:0, C16:1 $\omega$ 7 *cis*, and C18:1 $\omega$ 7 *cis*) contribute 42% to the total PLFA composition in the  
885 feces. If Synallactes hosted a large community of living bacteria, we would expect to detect a  
886 significant amount of bacteria-specific PLFAs in the gut content and a higher level of  
887 heterotrophic re-synthesis of amino acids. Additionally, the mean  $\delta^{15}\text{N}_{\text{source AA}}$ -value of its body-  
888 wall tissue would likely be enriched compared to the mean  $\delta^{15}\text{N}_{\text{source AA}}$ -value across all species.  
889 Therefore, we assume that Synallactidae gen sp. has a mixed diet consisting of foraminiferans,  
890 bacteria, and phytodetritus.

891

892 *Galatheathuria* 1om the **family Synallactidae** has an estimated trophic level of 3.1 and a  
893 medium level of heterotrophic re-synthesis of amino acids. Like Synallactidae gen sp., it feeds  
894 extremely selectively) and *Galatheathuria* sp. seems to consume preferably diatom-derived  
895 phytodetritus.

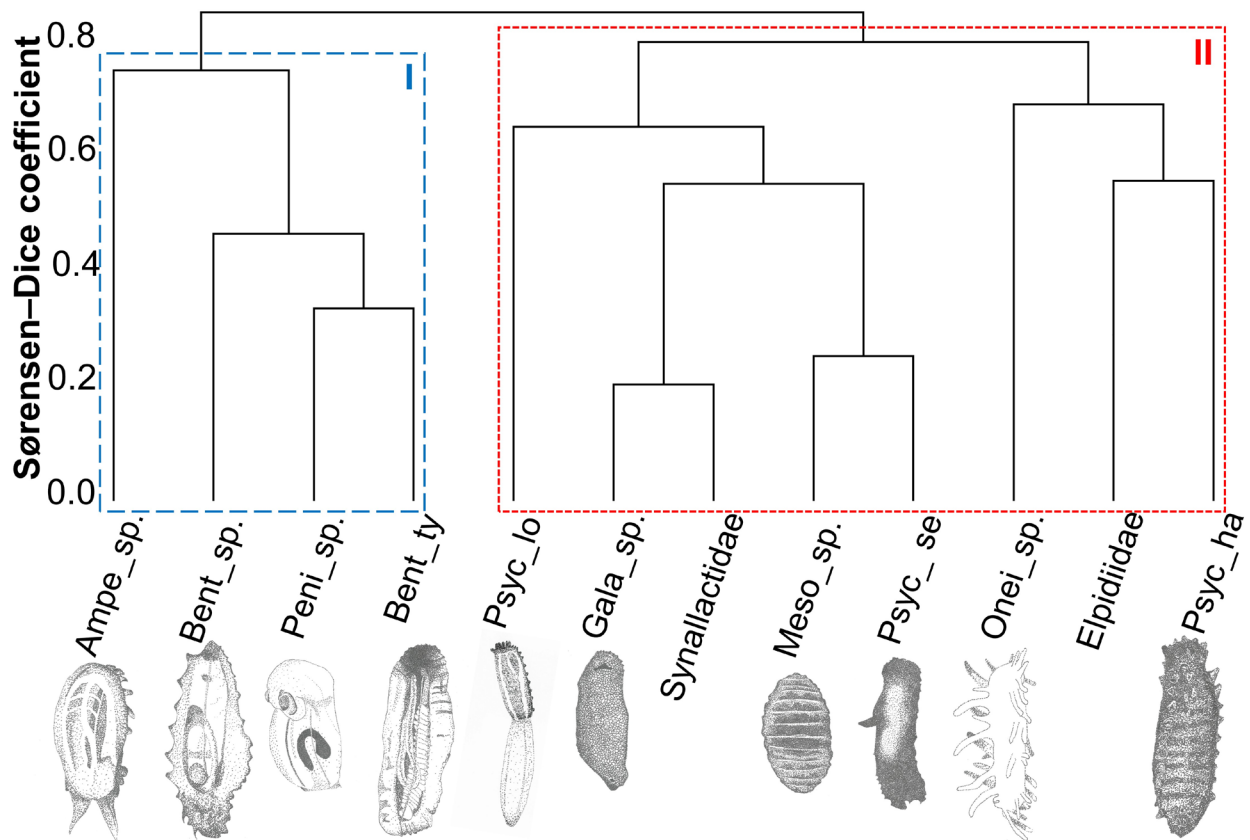
896

### 897 **Classification of holothurian trophic groups**

898 Here, we propose a classification system of trophic groups for holothurians from the Peru Basin  
899 (Fig. 11). It is based on cluster analysis of trophic levels, heterotrophic re-synthesis level of  
900 amino acids, feeding selectivity, and diet preferences. Trophic group 1 has a narrow trophic level  
901 between 2.7 and 2.9, feeds either very selectively or unselectively on phytodetritus and  
902 sedimentary detritus. Though, not statistically confirmed, we suggest splitting this trophic group  
903 1 in two subgroups: Trophic group 1a includes the very selectively feeding *Amperima* sp. with its  
904 dinoflagellate-derived detritus diet and trophic group 1b comprises the unselective feeders  
905 *Benthodytes* sp., *B. typica*, and *Peniagone* sp. that consume diatom-derived phytodetritus and  
906 sedimentary detritus.

907 Trophic group 2, in comparison, has a very large trophic level range between 2.0 and 3.5. This  
908 trophic group could be split again into two subgroups: Trophic group 2a (*P. longicauda*,  
909 *Galatheathuria* sp., Synallactidae gen sp., *Mesothuria* sp., *P. semperiana*) has a trophic level  
910 between 3.0 and 3.4 and feeds extremely selectively on phytodetritus or on a mixed diet with  
911 phytodetritus, sedimentary detritus, and bacteria. Trophic group 2b consists of Elpidiidae gen sp.,  
912 *P. hanseni*, and *Oneirophanta* sp. that feed selectively on phytodetritus, foraminiferans,  
913 sedimentary detritus, and bacteria.

914



915 **Figure 11.** Dendrogram of the Sørensen–Dice coefficient calculated for holothurian species from  
 916 the Peru Basin based. Trophic group I includes *Amperima* sp. (Ampe\_sp.), *Benthodytes* sp.  
 917 (Bent\_sp.), *Peniagone* sp. (Peni\_sp.), and *Benthodytes typica* (Bent\_ty). Trophic group II  
 918 comprises *Psychropotes longicauda* (Psyc\_lo), *Galatheathuria* sp. (Gala\_sp.), Synallactidae gen  
 919 sp. (Synallactidae), *Mesothuria* sp. (Meso\_sp.), *Psychropotes semperiana* (Psyc\_se),  
 920 *Oneirophanta* sp. (Onei\_sp.), Elpidiidae gen sp. (Elpidiidae), and *Psychronaetes hanseni*  
 921 (Psyc\_ha). Illustrations of holothurians by Tanja Stratmann.

922  
 923  
 924 **Potential resource partitioning and its importance for holothurian biodiversity in the Peru**  
 925 **Basin**

926 With 23 different holothurian morphotypes observed, the holothurian biodiversity in the abyssal  
 927 plain of the Peru Basin is higher than in the abyssal plains around the Bullard Fracture Zone and  
 928 the South Orkney Islands (Southern Ocean; Ogawa et al. 2022), the abyssal central Cantabrian  
 929 Sea (NE Atlantic; Fernández-Rodríguez et al. 2019), the abyssal Aleutian Basin (Bering Sea, NE  
 930 Pacific; Sigwart et al. 2023) and at PAP (Iken et al. 2001), but lower than at Station M (NE  
 931 Pacific; Kuhnz et al. 2020) and in the Clarion-Clipperton Fracture Zone (CCZ, central N Pacific;  
 932 Simon-Lledó et al. 2023a, b). The co-existence of so many deposit-feeding species of the same  
 933 taxonomic class is astonishing, as one might expect a strong competition among the different  
 934 taxa leading ultimately to taxa being outcompeted.

935 In the 1970s, Menge and Sutherland (1976) synthesized that high local species diversity is  
 936 maintained by predation (i.e., predation hypothesis; Paine 1966, 1971) and competition (i.e.,  
 937 competition hypothesis; Dobzhansky 1950). To reduce this interspecific competition, similar

938 species may subdivide their use of the available food sources (Schoener 1974; Winemiller and  
939 Pianka 1990), a process known as resource partitioning. Such resource partitioning along a  
940 decomposition gradient of food sources likely accounts for the high diversity of detritivores in  
941 soils (Schneider et al. 2004; Chahartaghi et al. 2005; Hishi et al. 2007). In an experiment with  
942 shallow-water benthic deposit-feeding echinoderms (i.e., holothurians and echinoids), however,  
943 species-specific traits and not resource partitioning explained the co-occurrence of species of the  
944 same feeding guild (Godbold et al. 2009).

945 The high holothurian biodiversity in the Peru Basin, in contrast, seems to be maintained by a  
946 combination of resource partitioning and particular selectivity, likely due to species-specific  
947 traits, such as different tentacle morphology (Roberts and Moore 1997; Pierrat et al. 2022),  
948 feeding rates and gut residence time (Godbold et al. 2009; Durden et al. 2020), and/ or mobility  
949 (Smith et al. 1993; Kaufmann and Smith 1997; Miguez-Salas et al. 2020). For instance,  
950 *Amperima* sp. as the only member of trophic group 1a ('Classification of holothurian trophic  
951 groups') moves non-randomly (Bluhm and Gebruk 1999) in a uniform direction with a mean  
952 speed of  $3.3 \pm 1.8$  cm hr<sup>-1</sup> (Wigham 2002). It moves mostly slowly and is stationary only 22% of  
953 the time (Wigham 2002). In fact, at PAP, *A. rosea* had a 20 times higher tracking rate between  
954 1997 and 1998 than the other holothurians present (Bett et al. 2001). As *Amperima* sp. shares the  
955 same tentacle structure (peltate) with *Benthodytes* sp. and *P. longicauda* (Roberts et al. 2000), we  
956 hypothesize, that indeed, mobility is the specific trait that enables this species to create its own  
957 feeding niche and to partition its food sources from the resources of the other holothurian  
958 species.

959 In comparison, the member of trophic group 1b *Peniagone* sp. can swim (Stratmann, personal  
960 observation; Pawson and Foell 1986; Bluhm and Gebruk 1999; Gong et al. 2020) and it was  
961 estimated that *Peniagone leander* Pawson & Foell, 1986, spends about half of its time at the  
962 seafloor and the other half swimming within 50 m above the seafloor (Pawson and Foell 1986).  
963 At the seafloor, *Peniagone vitrea* Théel, 1882 moves with  $8.1 \pm 7.9$  cm hr<sup>-1</sup> (Smith et al. 1993) to  
964  $10.1 \pm 12.9$  cm hr<sup>-1</sup> (Kaufmann and Smith 1997) in a 'running pattern' (frequency of records:  
965 46%) and in large loops (39%) (Kaufmann and Smith 1997). The species is therefore faster than  
966 *Amperima* sp., but slower than *O. mutabilis mutabilis* ( $64.6 \pm 68.4$  cm hr<sup>-1</sup>) and *Synallactes*  
967 *profundi* (Koehler & Vaney, 1905) ( $12.7 \pm 11.9$  cm hr<sup>-1</sup>) (Kaufmann and Smith 1997).  
968 *Peniagone* sp. has simple peltate tentacles (Roberts et al. 2000) and uses selective ingestion as  
969 primary feeding strategy (Purinton et al. 2008). Hence, in the Peru Basin this species probably  
970 co-occurs with the other holothurians due to its specific mobility trait and its selectivity.

971 *P. longicauda* as an example of trophic group 2a moves at the seafloor with a speed of 2.6 cm hr<sup>-1</sup>  
972 (Wigham 2002) and it may be able to 'sail' using its velum (Gebruk 1995). This species has  
973 peltate tentacles (Roberts and Moore 1997) and a complex gut system with a more extended  
974 pharynx and rectum compared to *Oneirophanta* sp. and *M. villosus* (Théel, 1886) (Moore et al.  
975 1995). This type of gut system might function as a mixing chamber (Penry and Jumars 1987) in  
976 which fermentation occurs (Roberts et al. 2000). Following that line of thought, the pattern we  
977 see in our data might not show extreme selectivity of food sources, but very efficient  
978 fermentation. However, as Khripounoff and Sibuet (1980) found a four times enrichment of  
979 organic C in the particles in *P. longicauda*'s pharynx compared to the ambient sediment, we  
980 propose that in the Peru Basin this species combines selective feeding with efficient  
981 fermentation.

982 *Oneirophanta* sp. (trophic group 2b) is the fastest holothurian species in this study and moves  
983 non-randomly with a speed of  $84.8 \pm 80.9$  cm hr<sup>-1</sup> (Smith et al. 1993) to  $128.9 \pm 68.3$  cm hr<sup>-1</sup>

984 (Smith et al. 1997) in a ‘running pattern’ (frequency of records: 60%) (Kaufmann and Smith  
985 1997). With its digitate tentacles (Roberts and Moore 1997) and its fast locomotion,  
986 *Oneirophanta* sp. is adapted to exploit fast fresh phytodetritus (Roberts et al. 2000; Witbaard et  
987 al. 2001; Wigham et al. 2003a) and replaces its gut content completely every 5 d (Witbaard et al.  
988 2001). When *P. longicauda* and *Oneirophanta* sp. co-occur like in the Peru Basin, *Oneirophanta*  
989 sp. outcompetes *P. longicauda* when fresh phytodetritus is available, but when fresh/ labile  
990 detritus is rare, both species compete for the same material (Neto et al. 2006; FitzGeorge-Balfour  
991 et al. 2010).

992 Hence, we suggest that the high biodiversity of holothurians in the Peru Basin is maintained by  
993 differences in species-specific traits (i.e., mobility, tentacle morphology, gut structure) which  
994 allow resource partitioning and selectivity.

995

### 996 **The effect of holothurians on sedimentary organic carbon availability in the Peru Basin**

997 Nine of the 13 species analyzed in this study were detected visually in an area of the Peru Basin  
998 that Stratmann et al. (2018b) called ‘reference site’. There, they had a density of  $157 \pm 9$  ind. ha<sup>-1</sup>  
999 (Stratmann et al. 2018b) and contributed 65% to total holothurian density in the Peru Basin. For  
1000 a subgroup of these species for which data on gut contents (Table 5) and densities (Stratmann et  
1001 al. 2018b) were available, it was possible to calculate the gut sediment stock. Together,  
1002 *Amperima* sp., *Benthodytes* sp., Elpidiidae gen sp., *Oneirophanta* sp., *Peniagone* sp., *P. hanseni*,  
1003 and *Synallactes* sp. (morphotype "pink") hold a gut sediment stock of 0.02 g DM gut content m<sup>-2</sup>.  
1004 In comparison, in the Santa Catalina Basin (NE Pacific) the three dominant surface deposit  
1005 feeders *Pannychia moseleyi* Théel, 1882 (holothurian), *Chiridota* sp. Eschscholtz, 1829  
1006 (holothurian), and *Bathybembix bairdii* Dall, 1889 (gastropod) have a gut standing stock of  
1007 0.27 g DM gut content m<sup>-2</sup> (Miller et al. 2000). Even though, it seems as if the holothurians in  
1008 the Peru Basin have a very small gut sediment stock, the species used to calculate the stocks  
1009 include only one (*Amperima* sp.) of the three dominant holothurian species in the Peru Basin.  
1010 Therefore, a direct comparison of these two datasets is not possible, but it is likely that the gut  
1011 sediment stock of holothurians in the Peru Basin is comparable to the gut sediment stock of the  
1012 dominant surface deposit feeders in the Santa Catalina Basin.

1013

1014 Based on the sediment stocks, it is possible to estimate sediment ingestion rates and upscale how  
1015 much of the sediment in the Peru Basin is bioturbated by 65% of all holothurians. Unfortunately,  
1016 we lacked information about gut residence times (GRTs) for most holothurian species for which  
1017 we had gut sediment stock data. Therefore, we approximated min and max ranges of sediment  
1018 ingestion rates by applying the same GRTs that were used previously in the literature (min<sub>GRT</sub> =  
1019 1 d, Miller et al. 2000; max<sub>GRT</sub> = 6 d, Lauerma et al. 1997) and multiplying it with a gut  
1020 sediment stock of 0.02 g DM gut content m<sup>-2</sup>. Hence, 65% of the holothurians reworked between  
1021 1.2 and 7.3 g DM sediment m<sup>-2</sup> yr<sup>-1</sup>. In comparison, the shallow-water tropical coral reef  
1022 holothurians *Holothuria atra* Jaeger, 1833, and *Stichopus chloronotus* Brandt, 1835, consume  
1023 4.6 kg DM sediment m<sup>-2</sup> yr<sup>-1</sup> at Lizard Island (Great Barrier Reef, Australia, SW Pacific) which  
1024 implies they bioturbate all the sediment in the upper 5 mm (Uthicke 1999). *Holothuria scabra*  
1025 Jaeger, 1833, populations in Fiji (SW Pacific) even ingest 10.5 kg DM sediment m<sup>-2</sup> yr<sup>-1</sup> (Lee et  
1026 al. 2018) and in W Australia *Holothuria whitmaei* Bell, 1887, ingests yearly between 2 and 14%  
1027 of all the available sediment (0–5 mm sediment depth) in 1 ha (Shiell and Knott 2010).

1028

1029 It was estimated that *P. moseleyi*, *Chiridota* sp., and *B. bairdii* process 39–52% of the daily  
1030 particulate organic carbon (POC) flux to the Santa Catalina Basin (Miller et al. 2000), whereas at  
1031 Station M, mobile invertebrate megabenthos including holothurians could process 0.2 to 4% of  
1032 the daily POC flux that reaches the seafloor (Smith et al. 1993; Lauerma et al. 1997). Hence, an  
1033 estimated ingestion of 4 to 27% of the daily POC flux to the Peru Basin ( $1.3 \text{ mg C m}^{-2} \text{ d}^{-1}$ ;  
1034 Hoving et al. 2023) by 65% of the holothurian community seems reasonable.  
1035 Not all the organic material that holothurians ingest is assimilated. Instead, a substantial fraction  
1036 is egested as feces. In fact, the fecal cast of a holothurian in the *in-situ* experiment still contained  
1037  $0.036 \text{ mmol phytodetritus C g}^{-1} \text{ DM feces}$  and  $0.028 \text{ mmol phytodetritus N g}^{-1} \text{ DM feces}$  from  
1038 the *S. costatum* with which it was fed. Also, in the Nazaré canyon, the faecal casts of *M.*  
1039 *musculus* still contained  $4.04 \pm 0.61 \text{ mg biopolymeric C g}^{-1} \text{ DM sediment}$  (Amaro et al. 2010).  
1040 Hence, holothurians increase the patchiness of organic C distribution in abyssal marine surface  
1041 sediments by producing fecal casts which, in theory, could be an important food source for  
1042 detritivores/ coprophagous feeders. However, a time-lapse camera study in 1978 showed that the  
1043 fecal cast of a holothurian was still distinguishable after 202 d (Paul et al. 1978) pointing towards  
1044 a low number of abyssal coprophagous feeders that target holothurian fecal casts.  
1045

### 1046 **Dependence of holothurians on fresh phytodetritus**

1047 In the *in-situ* experiment, the holothurians assimilated the *S. costatum*-derived PLFAs C14:0,  
1048 C16:0, C16:1 $\omega$ 7 *cis*, and EPA (Volkman et al. 1989; Table S5), whereas the largest fraction of  
1049  $^{13}\text{C}$ -PLFAs and  $^{13}\text{C}$ -NLFAs (PLFAs: 32–59%; NLFAs: 27–42%; Fig. 9) was C22:1 $\omega$ 9 *cis*. This  
1050 fatty acid was not present in *S. costatum* (Table S5), but it can be biosynthesized via carbon-  
1051 chain elongation of the precursor C18:1 $\omega$ 9 *cis* (Ackman and Castell 1966) which existed in *S.*  
1052 *costatum* (Table S5). However, the ecologically/ physiologically most interesting  $^{13}\text{C}$ -PLFA and  
1053  $^{13}\text{C}$ -NLFA is DPA, which was not detected in *S. costatum* (Table S5). This fatty acid is  
1054 biosynthesized from EPA via a two carbon-chain elongation (Mansour et al. 2005) and is used by  
1055 the shallow-water ophiuroid *Amphiura* (*Amphiura*) *elandiformis* A.M. Clark, 1966, to synthesize  
1056 DHA via  $\Delta$ 4 desaturation (Mansour et al. 2005). One of the *Amperima* sp. specimens in the *in-*  
1057 *situ* experiment was in fact able to biosynthesize DPA ( $0.080 \text{ nmol } ^{13}\text{C}\text{-PLFA mmol}^{-1} \text{ org. C}$ )  
1058 and DHA ( $0.019 \text{ nmol } ^{13}\text{C}\text{-PLFA mmol}^{-1} \text{ org. C}$ ) indicating that this biosynthetic pathway can be  
1059 performed by a broader range of taxonomic classes, including ophiuroids (Mansour et al. 2005),  
1060 asteroids (Jeffreys et al. 2009), holothurians (this study), arthropods (Jeffreys et al. 2009),  
1061 polychaetes (Jeffreys et al. 2009), and anthozoans (Jeffreys et al. 2009). Furthermore, it implies  
1062 that holothurians, or at least *Amperima* sp., are less dependent on ingesting all ‘essential’ fatty  
1063 acids with their food as they can biosynthesize DHA themselves when EPA is available.  
1064

1065 The ability of *Amperima* sp. to biosynthesize DHA from a precursor fatty acid might explain  
1066 why holothurians in the Peru Basin showed a net accumulation in this ‘essential’ fatty acid  
1067 (Fig. 10c), while they had a net deficiency in ARA. They could not remedy this deficiency in  
1068 ARA by ingesting fresh phytodetritus in the *in-situ* experiment because *S. costatum* did not  
1069 contain this specific fatty acid. Besides these ‘essential’ fatty acids, holothurians also had a net  
1070 deficiency in C16:0, C18:0, and C18:1 $\omega$ 1 *cis* (Fig. 10b). C16:0 and C18:1 $\omega$ 1 *cis* are fatty acids  
1071 that are present in bacteria (Table 1). Hence, a deficiency in these fatty acids could imply that  
1072 holothurians either did not ingest enough bacteria or bacteria-covered particles (Pierrat et al.

1073 2022), or that the microbiome in their guts did not produce these fatty acids in sufficient  
1074 quantities.  
1075 Holothurians from the Peru Basin had a net accumulation of most EAAs (leucine, phenylalanine,  
1076 threonine, valine), whereas the specimens from the *in-situ* experiment showed a net deficiency in  
1077 them. This indicates that these specific EAAs are not limited in the Peru Basin, but instead are  
1078 available in sufficient concentrations so that a pulse of fresh phytodetritus will likely not be  
1079 completely depleted.

1080  
1081 Holothurians are not only dependent on specific ‘essential’ fatty acids and EAAs that they have  
1082 to take up by grazing upon phytodetritus or biosynthesize partly themselves. They also depend  
1083 on phytodetritus containing the required chemical composition which changes depending on the  
1084 growth conditions of phytoplankton (Grosse et al. 2017, 2019). Already from 2000 to 2015 the  
1085 pelagic phytoplankton community has changed on a global scale with either a decrease in diatom  
1086 abundance, and/ or a change in the physiology of phytoplankton (Lorrain et al. 2020). For the  
1087 Peru Basin, no further changes in phytoplankton species richness are predicted for the period  
1088 from 2081 to 2100 (Benedetti et al. 2021), but less POC flux is predicted to reach the abyssal  
1089 seafloor in 2100 compared to present day conditions (Sweetman et al. 2017). This implies that  
1090 holothurians in the Peru Basin will be more dependent on pulses of fresh phytodetritus – though  
1091 not on *S. costatum* – in the future than at present day as the sediment will likely contain less  
1092 ‘essential’ fatty acids and EAAs that originated from surface primary producers and eventually  
1093 sank to the seafloor than now.

## 1094 1095 **Conclusion**

1096 This study identified feeding strategies and diet preferences of 13 putative holothurian species  
1097 from the Peru Basin which can be classified in two major trophic groups based on trophic level,  
1098 level of heterotrophic re-synthesis of amino acids, feeding selectivity, and diet preferences. The  
1099 differences in selectivity and resource partitioning were likely related to species-specific  
1100 variability in mobility, tentacle morphology, and gut structure, and allowed the high biodiversity  
1101 of holothurians in the abyssal plain of the Peru Basin. It was estimated that a subgroup of the  
1102 holothurian community is able to process between 4 and 27% of the daily POC flux and in doing  
1103 so, increases the heterogeneity of organic matter availability in the Peru Basin. Under current  
1104 conditions, holothurians are limited in the ‘essential’ fatty acid ARA, while at least one species  
1105 of the assemblage is able of biosynthesizing DHA from EPA. EAA are still available in  
1106 sufficient concentrations in the environment, but this might change in the future when less POC  
1107 flux reaches the abyssal plains.

1108  
1109 **Acknowledgements:** The authors thank chief scientist Prof. Antje Boetius, Dr. Felix Janssen, the  
1110 captain and crew of RV *Sonne*, and the ROV Kiel 6000 team from Geomar (Kiel) for their  
1111 excellent support during research cruise SO242-2. The authors thank furthermore Dr. Andrey  
1112 Gebruk for species identification of holothurians. Pieter van Rijswijk, Jana Stratmann, and Jonas  
1113 Sonntag are thanked for technical assistance during sample processing.

## 1114 1115 **References**

1116 Ackman RG (1989) Marine biogenic lipids, fats, and oils. CRC Press, Boca Raton, Florida

- 1117 Ackman RG, Castell JD (1966) Isomeric monoethylenic fatty acids in herring oil. *Lipids* 1:341–  
1118 348
- 1119 Alt CHS, Rogacheva A, Boorman B, et al (2013) Trawled megafaunal invertebrate assemblages  
1120 from bathyal depth of the Mid-Atlantic Ridge (48°-54°N). *Deep-Sea Research II* 98:326–  
1121 340. <https://doi.org/10.1016/j.dsr2.2013.02.003>
- 1122 Amaro T, Bianchelli S, Billett DSM, et al (2010) The trophic biology of the holothurian  
1123 *Molpadia musculus*: Implications for organic matter cycling and ecosystem functioning in a  
1124 deep submarine canyon. *Biogeosciences* 7:2419–2432. [https://doi.org/10.5194/bg-7-2419-](https://doi.org/10.5194/bg-7-2419-2010)  
1125 2010
- 1126 Benedetti F, Vogt M, Elizondo UH, et al (2021) Major restructuring of marine plankton  
1127 assemblages under global warming. *Nat Commun* 12:. [https://doi.org/10.1038/s41467-021-](https://doi.org/10.1038/s41467-021-25385-x)  
1128 25385-x
- 1129 Bett BJ, Malzone MG, Narayanaswamy BE, Wigham BD (2001) Temporal variability in  
1130 phytodetritus and megabenthic activity at the seabed in the deep Northeast Atlantic. *Prog*  
1131 *Oceanogr* 50:349–368. [https://doi.org/10.1016/S0079-6611\(01\)00066-0](https://doi.org/10.1016/S0079-6611(01)00066-0)
- 1132 Billett DSM (1991) Deep-sea holothurians. *Oceanography and Marine Biology* 29:259–317
- 1133 Billett DSM, Bett BJ, Reid WDK, et al (2010) Long-term change in the abyssal NE Atlantic: The  
1134 “Amperima Event” revisited. *Deep-Sea Research II* 57:1406–1417.  
1135 <https://doi.org/10.1016/j.dsr2.2009.02.001>
- 1136 Billett DSM, Bett BJ, Rice AL, et al (2001) Long-term change in the megabenthos of the  
1137 Porcupine Abyssal Plain (NE Atlantic). *Prog Oceanogr* 50:325–348.  
1138 [https://doi.org/10.1016/S0079-6611\(01\)00060-X](https://doi.org/10.1016/S0079-6611(01)00060-X)
- 1139 Bligh EG, Dyer WJ (1959) A rapid method of total lipid extraction and purification. *Can J*  
1140 *Biochem Physiol* 37:911–917. <https://doi.org/10.1139/o59-099>
- 1141 Bluhm H, Gebruk A V. (1999) Holothuroidea (Echinodermata) of the Peru Basin - ecological  
1142 and taxonomic remarks based on underwater images. *Marine Ecology* 20:167–195.  
1143 <https://doi.org/10.1046/j.1439-0485.1999.00072.x>
- 1144 Boetius A (2015) RV SONNE Fahrtbericht / Cruise Report SO242-2 [SO242/2]: JPI OCEANS  
1145 Ecological Aspects of Deep-Sea Mining, DISCOL Revisited, Guayaquil - Guayaquil  
1146 (Equador), 28.08.-01.10.2015.
- 1147 Boschker H (2008) Linking microbial community structure and functioning: Stable isotope  
1148 (<sup>13</sup>C) labeling in combination with PLFA analysis. *Molecular Microbial Ecology Manual II*  
1149 1673–1688. [https://doi.org/10.1007/978-1-4020-2177-0\\_807](https://doi.org/10.1007/978-1-4020-2177-0_807)
- 1150 Boschker HTS, de Brouwer JFC, Cappenberg TE (1999) The contribution of macrophyte-  
1151 derived organic matter to microbial biomass in salt-marsh sediments: Stable carbon isotope  
1152 analysis of microbial biomarkers. *Limnol Oceanogr* 44:309–319.  
1153 <https://doi.org/10.4319/lo.1999.44.2.0309>

- 1154 Brown A, Hauton C, Stratmann T, et al (2018) Metabolic rates are significantly lower in abyssal  
1155 Holothuroidea than in shallow-water Holothuroidea. *R Soc Open Sci* 5:172162.  
1156 <https://doi.org/10.1098/rsos.172162>
- 1157 Budge SM, Parrish CC (1998) Lipid biogeochemistry of plankton, settling matter and sediments  
1158 in Trinity Bay, Newfoundland. II. Fatty acids. *Org Geochem* 29:1547–1559
- 1159 Bühring SI, Koppelman R, Christiansen B, Weikert H (2002) Are Rhodophyceae a dietary  
1160 component for deep-sea holothurians? *Journal of the Marine Biological Association of the*  
1161 *United Kingdom* 82:347–348. <https://doi.org/10.1017/S0025315402005556>
- 1162 Chahartaghi M, Langel R, Scheu S, Ruess L (2005) Feeding guilds in Collembola based on  
1163 nitrogen stable isotope ratios. *Soil Biol Biochem* 37:1718–1725.  
1164 <https://doi.org/10.1016/j.soilbio.2005.02.006>
- 1165 Chikaraishi Y, Ogawa NO, Kashiya Y, et al (2009) Determination of aquatic food-web  
1166 structure based on compound-specific nitrogen isotopic composition of amino acids. *Limnol*  
1167 *Oceanogr Methods* 7:740–750. <https://doi.org/10.4319/lom.2009.7.740>
- 1168 Choi A, Song J, Joung Y, et al (2015) *Lentisphaera profunda* sp. nov., Isolated from deep-sea  
1169 water. *Int J Syst Evol Microbiol* 65:4186–4190. <https://doi.org/10.1099/ijsem.0.000556>
- 1170 Dalsgaard J, St. John M, Kattner G, et al (2003) Fatty acid trophic markers in the pelagic marine  
1171 environment. *Adv Mar Biol* 46:225–340. [https://doi.org/10.1016/S0065-2881\(03\)46005-7](https://doi.org/10.1016/S0065-2881(03)46005-7)
- 1172 Dice LR (1945) Measures of the amount of ecological association between species. *Ecology*  
1173 26:297–302
- 1174 Dobzhansky T (1950) Evolution in the tropics. *Am Sci* 38:208–221
- 1175 Durden JM, Bett BJ, Huffard CL, et al (2020) Response of deep-sea deposit-feeders to detrital  
1176 inputs: A comparison of two abyssal time-series sites. *Deep-Sea Research II* 173:104677.  
1177 <https://doi.org/10.1016/j.dsr2.2019.104677>
- 1178 Elvert M, Boetius A, Knittel K, Barker Jørgensen BO (2003) Characterization of Specific  
1179 Membrane Fatty Acids as Chemotaxonomic Markers for Sulfate-Reducing Bacteria  
1180 Involved in Anaerobic Oxidation of Methane. <https://doi.org/10.1080/01490450390241071>
- 1181 Engel N, Aguado MT, Maraun M (2023) Trophic ecology of three marine polychaete species:  
1182 Evidence from laboratory experiments using stable isotope (<sup>15</sup>N, <sup>13</sup>C), fatty acid (NLFA)  
1183 analyses, and C and N stoichiometry. *Mar Environ Res* 185:.  
1184 <https://doi.org/10.1016/j.marenvres.2023.105878>
- 1185 Erbe T (1999) Die Quantifizierung von Aminosäureisomeren in Lebensmitteln mittels chiraler  
1186 Gaschromatographie-Massenspektrometrie im Hinblick auf die Relevanz und die  
1187 Entstehungsmechanismen von D-Aminosäuren. Justus-Liebig-Universität Gießen
- 1188 Faergeman NJ, Knudsen J (1997) Role of long-chain fatty acyl-CoA esters in the regulation of  
1189 metabolism and in cell signalling. *Biochemical Journal* 323:1–12

- 1190 Falk-Petersen S, Sargent JR, Tande KS (1987) Lipid composition of zooplankton in relation to  
1191 the Sub-Arctic food web. *Polar Biol* 8:115–120
- 1192 Fernández-Rodríguez I, Arias A, Anadón N, Acuña JL (2019) Holothurian (Echinodermata)  
1193 diversity and distribution in the central Cantabrian Sea and the Avilés Canyon System (Bay  
1194 of Biscay). *Zootaxa* 4567:293–325
- 1195 Findlay RH, Trexler MB, Guckerte JB, White DC (1990) Laboratory study of disturbance in  
1196 marine sediments: response of a microbial community. *Mar Ecol Prog Ser* 62:121–133
- 1197 FitzGeorge-Balfour T, Billett DSM, Wolff GA, et al (2010) Phytopigments as biomarkers of  
1198 selectivity in abyssal holothurians; interspecific differences in response to a changing food  
1199 supply. *Deep-Sea Research II* 57:1418–1428. <https://doi.org/10.1016/j.dsr2.2010.01.013>
- 1200 Fry B (2006) *Stable Isotope Ecology*, 3rd edn. Springer New York, New York, NY
- 1201 Gausepohl F, Hennke A, Schoening T, et al (2020) Scars in the abyss: reconstructing sequence,  
1202 location and temporal change of the 78 plough tracks of the 1989 DISCOL deep-sea  
1203 disturbance experiment in the Peru Basin. *Biogeosciences* 17:1463–1493.  
1204 <https://doi.org/10.5194/bg-17-1463-2020>
- 1205 Gausepohl F, Hennke A, Schoening T, et al (2019) Bathymetric grid from the DISCOL working  
1206 area of SONNE cruise SO242/1 in the Peru Basin. *PANGAEA*
- 1207 Gebruk A V. (1995) Locomotory organs in the elaspodid holothurians: Functional-  
1208 morphological and evolutionary approaches. In: Emson R, Smith A, Campbell A (eds)  
1209 *Echinoderm Research*. Balkema, Rotterdam, pp 95–102
- 1210 Gelman A, Carlin JB, Stern HS, et al (2014) *Bayesian Data Analysis*. Chapman & Hall/ CRC,  
1211 Boca Raton, FL
- 1212 Gelman A, Rubin DB (1992) Inference from iterative simulation using multiple sequences.  
1213 *Statistical Science* 7:457–472. <https://doi.org/10.1214/ss/1177011136>
- 1214 Geweke J (1991) Evaluating the accuracy of sampling-based approaches to the calculation of  
1215 posterior moments. *Research Department Staff Report*, pp 1–30
- 1216 Ginger ML, Billett DSM, Mackenzie KL, et al (2001) Organic matter assimilation and selective  
1217 feeding by holothurians in the deep sea: Some observations and comments. *Prog Oceanogr*  
1218 50:407–421
- 1219 Ginger ML, Santos VLCS, Wolff GA (2000) A preliminary investigation of the lipids of abyssal  
1220 holothurians from the north-east Atlantic Ocean. *Journal of the Marine Biological*  
1221 *Association of the UK* 80:139–146. <https://doi.org/10.1017/s0025315499001654>
- 1222 Glencross BD (2009) Exploring the nutritional demand for essential fatty acids by aquaculture  
1223 species. *Aquac Res* 48:71–124. <https://doi.org/10.1111/J.1753-5131.2009.01006.X>

- 1224 Godbold JA, Rosenberg R, Solan M (2009) Species-specific traits rather than resource  
1225 partitioning mediate diversity effects on resource use. *PLoS One* 4:  
1226 <https://doi.org/10.1371/journal.pone.0007423>
- 1227 Gong L, Li X, Xiao N, et al (2020) Rediscovery of the abyssal species *Peniagone leander*  
1228 Pawson and Foell, 1986 (Holothuroidea: Elasipodida: Elpidiidae): The first record from the  
1229 Mariana Trench area. *J Oceanol Limnol* 38:1319–1327. [https://doi.org/10.1007/s00343-](https://doi.org/10.1007/s00343-020-0067-9)  
1230 [020-0067-9](https://doi.org/10.1007/s00343-020-0067-9)
- 1231 Graber S, Sumida C, Nunez E (1994) Fatty acids and cell signal transduction. *J Lipid Mediat*  
1232 *Cell Signal* 9:91–116
- 1233 Graeve M, Dauby P, Scailteur Y (2001) Combined lipid, fatty acid and digestive tract content  
1234 analyses: A penetrating approach to estimate feeding modes of Antarctic amphipods. *Polar*  
1235 *Biol* 24:853–862. <https://doi.org/10.1007/s003000100295>
- 1236 Grosse J, Brussaard CPD, Boschker HTS (2019) Nutrient limitation driven dynamics of amino  
1237 acids and fatty acids in coastal phytoplankton. *Limnol Oceanogr* 64:302–316.  
1238 <https://doi.org/10.1002/lno.11040>
- 1239 Grosse J, Burson A, Stomp M, et al (2017) From ecological stoichiometry to biochemical  
1240 composition: Variation in N and P supply alters key biosynthetic rates in marine  
1241 phytoplankton. *Front Microbiol* 8:. <https://doi.org/10.3389/fmicb.2017.01299>
- 1242 Grupe B, Becker HJ, Oebius HU (2001) Geotechnical and sedimentological investigations of  
1243 deep-sea sediments from a manganese nodule field of the Peru Basin. *Deep-Sea Research II*  
1244 48:3593–3608. [https://doi.org/10.1016/S0967-0645\(01\)00058-3](https://doi.org/10.1016/S0967-0645(01)00058-3)
- 1245 Gutiérrez MH, Vera J, Srain B, et al (2020) Biochemical fingerprints of marine fungi:  
1246 Implications for trophic and biogeochemical studies. *Aquatic Microbial Ecology* 84:75–90.  
1247 <https://doi.org/10.3354/ame01927>
- 1248 Hishi T, Hyodo F, Saitoh S, Takeda H (2007) The feeding habits of collembola along  
1249 decomposition gradients using stable carbon and nitrogen isotope analyses. *Soil Biol*  
1250 *Biochem* 39:1820–1823. <https://doi.org/10.1016/j.soilbio.2007.01.028>
- 1251 Hoving H-J, Boetius A, Dunlop K, et al (2023) Major fine-scale spatial heterogeneity in  
1252 accumulation of gelatinous carbon fluxes on the deep seabed. *Front Mar Sci* 10:1192242.  
1253 <https://doi.org/10.3389/fmars.2023.1192242>
- 1254 Hudson IR, Pond DW, Billett DSM, et al (2004) Temporal variations in fatty acid composition of  
1255 deep-sea holothurians: evidence of benthic-pelagic coupling. *Mar Ecol Prog Ser* 281:109–  
1256 120
- 1257 Hudson IR, Wigham BD, Billett DSM, Tyler PA (2003) Seasonality and selectivity in the  
1258 feeding ecology and reproductive biology of deep-sea bathyal holothurians. *Prog Oceanogr*  
1259 59:381–407. <https://doi.org/10.1016/j.pocean.2003.11.002>

- 1260 Hudson IR, Wigham BD, Solan M, Rosenberg R (2005) Feeding behaviour of deep-sea dwelling  
1261 holothurians: Inferences from a laboratory investigation of shallow fjordic species. *Journal*  
1262 *of Marine Systems* 57:201–218. <https://doi.org/10.1016/j.jmarsys.2005.02.004>
- 1263 Iken K, Brey T, Wand U, et al (2001) Food web structure of the benthic community at the  
1264 Porcupine Abyssal Plain (NE Atlantic): a stable isotope analysis. *Prog Oceanogr* 50:383–  
1265 405
- 1266 Jarman CL, Larsen T, Hunt T, et al (2017) Diet of the prehistoric population of Rapa Nui (Easter  
1267 Island, Chile) shows environmental adaptation and resilience. *Am J Phys Anthropol*  
1268 164:343–361. <https://doi.org/10.1002/ajpa.23273>
- 1269 Jeffreys RM, Wolff GA, Murty SJ (2009) The trophic ecology of key megafaunal species at the  
1270 Pakistan Margin: Evidence from stable isotopes and lipid biomarkers. *Deep Sea Res 1*  
1271 *Oceanogr Res Pap* 56:1816–1833. <https://doi.org/10.1016/j.dsr.2009.05.001>
- 1272 Kassambara A, Mundt F (2020) factoextra: Extract and Visualize the Results of Multivariate  
1273 Data Analyses
- 1274 Kaufmann RS, Smith KL (1997) Activity patterns of mobile epibenthic megafauna at an abyssal  
1275 site in the eastern North Pacific : Results from a 17-month time-lapse photographic study.  
1276 *Deep-Sea Research I* 44:559–579
- 1277 Kharlamenko VI (2018) Abyssal foraminifera as the main source of rare and new  
1278 polyunsaturated fatty acids in deep-sea ecosystems. *Deep-Sea Research II* 154:358–364.  
1279 <https://doi.org/10.1016/j.dsr2.2017.10.015>
- 1280 Kharlamenko VI, Zhukova N V, Khotimchenko S V, et al (1995) Fatty acids as markers of food  
1281 sources in a shallow-water hydrothermal ecosystem (Kraternaya Bight, Yankich Island,  
1282 Kurile Islands). *Mar Ecol Prog Ser* 120:231–241
- 1283 Khripounoff A, Sibuet M (1980) La nutrition d'échinodermes abyssaux. I. Alimentation des  
1284 holothuries. *Mar Biol* 60:17–26
- 1285 Koleff P, Gaston KJ, Lennon JJ (2003) Measuring beta diversity for presence-absence data.  
1286 *Journal of Animal Ecology* 72:367–382. <https://doi.org/10.1046/j.1365-2656.2003.00710.x>
- 1287 Kuhnz LA, Ruhl HA, Huffard CL, Smith KL (2020) Benthic megafauna assemblage change over  
1288 three decades in the abyss: Variations from species to functional groups. *Deep Sea Res 2*  
1289 *Top Stud Oceanogr* 173:. <https://doi.org/10.1016/j.dsr2.2020.104761>
- 1290 Kurkiewicz S, Dzierzewicz Z, Wilczok T, Dworzanski JP (2003) GC/MS determination of fatty  
1291 acid picolinyl esters by direct Curie-point pyrolysis of whole bacterial cells. *J Am Soc Mass*  
1292 *Spectrom* 14:58–62. [https://doi.org/10.1016/S1044-0305\(02\)00817-6](https://doi.org/10.1016/S1044-0305(02)00817-6)
- 1293 Larkin KE, Gooday AJ, Woulds C, et al (2014) Uptake of algal carbon and the likely synthesis of  
1294 an “essential” fatty acid by *Uvigerina* ex. gr. *semiornata* (Foraminifera) within the Pakistan  
1295 margin oxygen minimum zone: Evidence from fatty acid biomarker and <sup>13</sup>C tracer  
1296 experiments. *Biogeosciences* 11:3729–3738. <https://doi.org/10.5194/bg-11-3729-2014>

- 1297 Lauerman LML, Smoak JM, Shaw TJ, et al (1997) 234Th and 210Pb evidence for rapid  
1298 ingestion of settling particles by mobile epibenthic megafauna in the abyssal NE Pacific.  
1299 *Limnol Oceanogr* 42:589–595. <https://doi.org/10.4319/lo.1997.42.3.0589>
- 1300 Lee S, Ford AK, Mangubhai S, et al (2018) Effects of sandfish (*Holothuria scabra*) removal on  
1301 shallow-water sediments in Fiji. *PeerJ* 2018:. <https://doi.org/10.7717/peerj.4773>
- 1302 Libes S (2009) Introduction to marine biogeochemistry, 2nd edn. Academic Press, Inc.,  
1303 Burlington
- 1304 Lindsay DB (1975) Fatty acids as energy sources. *Proceedings of the Nutrition Society* 34:241–  
1305 248. <https://doi.org/10.1079/pns19750045>
- 1306 Lorrain A, Pethybridge H, Cassar N, et al (2020) Trends in tuna carbon isotopes suggest global  
1307 changes in pelagic phytoplankton communities. *Glob Chang Biol* 26:458–470.  
1308 <https://doi.org/10.1111/gcb.14858>
- 1309 Lovern J (1935) Fat metabolism in fishes: The fats of some plankton crustacea. *Biochemical*  
1310 *Journal* 29:847–849
- 1311 Lüdecke D, Ben-Shachar M, Patil I, Makowski D (2020) Extracting, Computing and Exploring  
1312 the Parameters of Statistical Models using R. *J Open Source Softw* 5:2445.  
1313 <https://doi.org/10.21105/joss.02445>
- 1314 Maier SR, Kutti T, Bannister RJ, et al (2019) Survival under conditions of variable food  
1315 availability: Resource utilization and storage in the cold-water coral *Lophelia pertusa*.  
1316 *Limnol Oceanogr* 64:1651–1671. <https://doi.org/10.1002/lno.11142>
- 1317 Mansour MP, Holdsworth DG, Forbes SE, et al (2005) High contents of 24:6(n-3) and 20:1(n-  
1318 13) fatty acids in the brittle star *Amphiura elandiformis* from Tasmanian coastal sediments.  
1319 *Biochem Syst Ecol* 33:659–674. <https://doi.org/10.1016/j.bse.2004.12.011>
- 1320 Marchig V, Von Stackelberg U, Hufnagel H, Durn G (2001) Compositional changes of surface  
1321 sediments and variability of manganese nodules in the Peru Basin
- 1322 Marsay CM, Sanders RJ, Henson SA, et al (2015) Attenuation of sinking particulate organic  
1323 carbon flux through the mesopelagic ocean. *Proceedings of the National Academy of*  
1324 *Sciences* 112:1089–1094. <https://doi.org/10.1073/pnas.1415311112>
- 1325 Massin C (1982) Food and feeding mechanisms: Holothuroidea. In: Jangoux M, Lawrence JM  
1326 (eds) *Echinoderm Nutrition*. Balkema, Rotterdam, pp 43–55
- 1327 McCarthy MD, Benner R, Lee C, Fogel ML (2007) Amino acid nitrogen isotopic fractionation  
1328 patterns as indicators of heterotrophy in plankton, particulate, and dissolved organic matter.  
1329 *Geochim Cosmochim Acta* 71:4727–4744. <https://doi.org/10.1016/j.gca.2007.06.061>
- 1330 McClelland JW, Montoya JP (2002) Trophic relationships and the nitrogen isotopic composition  
1331 of amino acids in plankton. *Ecology* 83:2173–2180. [https://doi.org/10.1890/0012-9658\(2002\)083\[2173:TRATNI\]2.0.CO;2](https://doi.org/10.1890/0012-9658(2002)083[2173:TRATNI]2.0.CO;2)

- 1333 Menge BA, Sutherland JP (1976) Species diversity gradients: Synthesis of the roles of predation,  
1334 competition, and temporal heterogeneity. *Am Nat* 110:351–369
- 1335 Mevenkamp L, Guilini K, Boetius A, et al (2019) Responses of an abyssal meiobenthic  
1336 community to short-term burial with crushed nodule particles in the South-East Pacific.  
1337 *Biogeosciences* 16:2329–2341. <https://doi.org/10.5194/bg-16-2329-2019>
- 1338 Middelburg JJ, Barranguet C, Boschker HTS, et al (2000) The fate of intertidal  
1339 microphytobenthos carbon: An *in situ* <sup>13</sup>C-labeling study. *Limnol Oceanogr* 45:1224–1234.  
1340 <https://doi.org/10.4319/lo.2000.45.6.1224>
- 1341 Miguez-Salas O, Huffard CL, Smith KL, et al (2020) Faunal assemblage changes, bioturbation  
1342 and benthic storms at an abyssal station in the northeastern Pacific. *Deep Sea Res 1*  
1343 *Oceanogr Res Pap* 160:. <https://doi.org/10.1016/j.dsr.2020.103277>
- 1344 Miller RJ, Smith CR, Demaster DJ, Fornes WL (2000) Feeding selectivity and rapid particle  
1345 processing by deep-sea megafaunal deposit feeders: A <sup>234</sup>Th tracer approach. *J Mar Res*  
1346 58:653–673
- 1347 Moore H, Manship B, Roberts D (1995) Gut structure and digestive strategies in three species of  
1348 abyssal holothurians. In: *Echinoderm Research*. Balkema, Rotterdam, pp 111–119
- 1349 Neto RR, Wolff GA, Billett DSM, et al (2006) The influence of changing food supply on the  
1350 lipid biochemistry of deep-sea holothurians. *Deep-Sea Research I* 53:516–527.  
1351 <https://doi.org/10.1016/j.dsr.2005.12.001>
- 1352 Nomaki H, Ogawa NO, Ohkouchi N, et al (2008) Benthic foraminifera as trophic links between  
1353 phytodetritus and benthic metazoans: Carbon and nitrogen isotopic evidence. *Mar Ecol Prog*  
1354 *Ser* 357:153–164. <https://doi.org/10.3354/meps07309>
- 1355 Ogawa A, Jimi N, Hiruta SF, et al (2022) Taxonomy and distribution of deep benthos collected  
1356 in and around the Southern Ocean during the 30th Anniversary expeditions of R/V Hakuho  
1357 Maru: Annelida, Mollusca, Ostracoda, Decapoda, and Echinodermata. *Polar Sci* 32:.  
1358 <https://doi.org/10.1016/j.polar.2022.100846>
- 1359 Oksanen J, Blanchet FG, Friendly M, et al (2017) *vegan*: Community ecology package.
- 1360 Pagès A, Grice K, Ertefai T, et al (2014) Organic geochemical studies of modern microbial mats  
1361 from Shark Bay: Part I: Influence of depth and salinity on lipid biomarkers and their  
1362 isotopic signatures. *Geobiology* 12:469–487. <https://doi.org/10.1111/gbi.12094>
- 1363 Paine RT (1966) Food web complexity and species diversity. *Am Nat* 100:65–75
- 1364 Paine RT (1971) A short-term experimental investigation of resource partitioning in a New  
1365 Zealand rocky intertidal habitat. *Ecology* 52:1096–1106
- 1366 Parrish CC, Thompson RJ, Deibel D (2005) Lipid classes and fatty acids in plankton and settling  
1367 matter during the spring bloom in a cold ocean coastal environment. *Mar Ecol Prog Ser*  
1368 286:57–68

- 1369 Paul AZ, Thorndike EM, Sullivan LG, et al (1978) Observations of the deep-sea floor from 202  
1370 days of time-lapse photography. *Nature* 272:812–814
- 1371 Paul SALL, Gaye B, Haeckel M, et al (2018) Biogeochemical regeneration of a nodule mining  
1372 disturbance site: Trace metals, DOC and amino acids in deep-sea sediments and pore  
1373 waters. *Front Mar Sci* 5:1–17. <https://doi.org/10.3389/fmars.2018.00117>
- 1374 Pawson DL, Foell EJ (1986) *Peniagone leander* new species, an abyssal benthopelagic sea  
1375 cucumber (Echinodermata: Holothuroidea) from the eastern central Pacific Ocean. *Bull Mar*  
1376 *Sci* 38:293–299
- 1377 Penry DL, Jumars PA (1987) Modeling animal guts as chemical reactors. *Am Nat* 129:69–96
- 1378 Phillips NW (1984) Role of different microbes and substrates as potential suppliers of specific,  
1379 essential nutrients to marine detritivores. *Bull Mar Sci* 35:283–298
- 1380 Pierrat J, Bédier A, Eeckhaut I, et al (2022) Sophistication in a seemingly simple creature: a  
1381 review of wild holothurian nutrition in marine ecosystems. *Biological Reviews* 97:273–298.  
1382 <https://doi.org/10.1111/brv.12799>
- 1383 Purinton BL, DeMaster DJ, Thomas CJ, Smith CR (2008)  $^{14}\text{C}$  as a tracer of labile organic  
1384 matter in Antarctic benthic food webs. *Deep-Sea Research II* 55:2438–2450.  
1385 <https://doi.org/10.1016/j.dsr2.2008.06.004>
- 1386 Qi H, Coplen TB, Mroczkowski SJ, et al (2016) A new organic reference material, l -glutamic  
1387 acid, USGS41a, for  $\delta^{13}\text{C}$  and  $\delta^{15}\text{N}$  measurements – a replacement for USGS41. *Rapid*  
1388 *Communications in Mass Spectrometry* 30:859–866
- 1389 Qui H, Coplen TB, Geilmann H, et al (2004) Two new organic reference materials for  $\delta^{13}\text{C}$  and  
1390  $\delta^{15}\text{N}$  measurements and a new value for the  $\delta^{13}\text{C}$  of NBS 22 oil. *Rapid Communications in*  
1391 *Mass Spectrometry* 17:2483–2487
- 1392 R-Core Team (2022) R: A language and environment for statistical computing
- 1393 Riebesell U, Schulz KG, Bellerby RGJ, et al (2007) Enhanced biological carbon consumption in  
1394 a high  $\text{CO}_2$  ocean. *Nature* 450:545–548. <https://doi.org/10.1038/nature06267>
- 1395 Roberts D, Gebruk A, Levin V, Manship BAD (2000) Feeding and digestive strategies in  
1396 deposit-feeding holothurians. *Oceanography and Marine Biology: An annual review*  
1397 38:257–310
- 1398 Roberts D, Moore HM (1997) Tentacular diversity in deep-sea deposit-feeding holothurians:  
1399 implications for biodiversity in the deep sea. *Biodivers Conserv* 6:1487–1505
- 1400 Romero-Romero S, Miller EC, Black JA, et al (2021) Abyssal deposit feeders are secondary  
1401 consumers of detritus and rely on nutrition derived from microbial communities in their  
1402 guts. *Sci Rep* 11:. <https://doi.org/10.1038/s41598-021-91927-4>
- 1403 Romesburg HC (1984) Cluster analysis for researschers. Lifetime Learning Publications

- 1404 Roy V (2020) Convergence diagnostics for Markov Chain Monte Carlo. *Annu Rev Stat Appl*  
1405 7:387–412. <https://doi.org/10.1146/annurev-statistics-031219>
- 1406 Ruhl HA (2007) Abundance and size distribution dynamics of abyssal epibenthic megafauna in  
1407 the northeast Pacific. *Ecology* 88:1250–1262. <https://doi.org/10.1890/06-0890>
- 1408 Sampath H, Ntambi JM (2004) Polyunsaturated fatty acid regulation of gene expression. *Nutr*  
1409 *Rev* 62:333–339. <https://doi.org/10.1301/nr.2004.sept.333-339>
- 1410 Sargent JR (1995) Origins and functions of n-3 polyunsaturated fatty acids in marine organisms.  
1411 In: *Proceedings of the 6th International Colloquium: Phospholipids: characterization,*  
1412 *metabolism, and novel biological applications.* pp 248–259
- 1413 Sargent JR, Falk-Petersen S. (1988) The lipid biochemistry of calanoid copepods. *Hydrobiology*  
1414 167/168:101–114
- 1415 Schneider K, Migge S, Norton RA, et al (2004) Trophic niche differentiation in soil  
1416 microarthropods (Oribatida, Acari): Evidence from stable isotope ratios ( $^{15}\text{N}/^{14}\text{N}$ ). *Soil*  
1417 *Biol Biochem* 36:1769–1774. <https://doi.org/10.1016/j.soilbio.2004.04.033>
- 1418 Schoener TW (1974) Resource partitioning in ecological communities. *Science* (1979) 185:27–  
1419 39
- 1420 Sharp Z (2017) *Principles of Stable Isotope Geochemistry*, 2nd edn. University of New Mexico,  
1421 Albuquerque
- 1422 Shiell GR, Knott B (2010) Aggregations and temporal changes in the activity and bioturbation  
1423 contribution of the sea cucumber *Holothuria whitmaei* (Echinodermata: Holothuroidea).  
1424 *Mar Ecol Prog Ser* 415:127–139. <https://doi.org/10.3354/meps08685>
- 1425 Sigwart JD, Brandt A, Di Franco D, et al (2023) Heterogeneity on the abyssal plains: A case  
1426 study in the Bering Sea. *Front Mar Sci* 9:. <https://doi.org/10.3389/fmars.2022.1037482>
- 1427 Simon-Lledó E, Amon DJ, Bribiesca-Contreras G, et al (2023a) Carbonate compensation depth  
1428 drives abyssal biogeography in the northeast Pacific. *Nat Ecol Evol.*  
1429 <https://doi.org/10.1038/s41559-023-02122-9>
- 1430 Simon-Lledó E, Amon DJ, Bribiesca-Contreras G, et al (2023b) Abyssal Pacific Seafloor  
1431 Megafauna Atlas. <https://doi.org/10.5281/ZENODO.8172728>
- 1432 Smith A, Matthiopoulos J, Priede IG (1997) Areal coverage of the ocean floor by the deep-sea  
1433 elaspodid holothurian *Oneirophanta mutabilis*: Estimates using systematic, random and  
1434 directional search strategy simulations. *Deep-Sea Research I* 44:477–486
- 1435 Smith CR, De Léo FC, Bernardino AF, et al (2008) Abyssal food limitation, ecosystem structure  
1436 and climate change. *Trends Ecol Evol* 23:518–528.  
1437 <https://doi.org/10.1016/j.tree.2008.05.002>

- 1438 Smith KL, Kaufmann RS, Wakefield WW (1993) Mobile megafaunal activity monitored with a  
1439 time-lapse camera in the abyssal North Pacific. *Deep-Sea Research I* 40:2307–2324.  
1440 [https://doi.org/10.1016/0967-0637\(93\)90106-D](https://doi.org/10.1016/0967-0637(93)90106-D)
- 1441 Sørensen T (1948) A method of establishing groups of equal amplitude in plant sociology based  
1442 on similarity of species content and its application to analysis of the vegetation on Danish  
1443 commons. Det Kongelige Danske Videnskabernes Selskab, Copenhagen
- 1444 Spector AA, Yorek MA (1985) Membrane lipid composition and cellular function. *J Lipid Res*  
1445 26:1015–1035
- 1446 Stock B, Semmens B, Ward E, et al (2020) MixSIAR: Bayesian Mixing Models in R
- 1447 Stock BC, Jackson AL, Ward EJ, et al (2018) Analyzing mixing systems using a new generation  
1448 of Bayesian tracer mixing models. *PeerJ* 2018:. <https://doi.org/10.7717/peerj.5096>
- 1449 Stratmann T, Mevenkamp L, Sweetman AK, et al (2018a) Has phytodetritus processing by an  
1450 abyssal soft-sediment community recovered 26 years after an experimental disturbance?  
1451 *Front Mar Sci* 5:1–13. <https://doi.org/10.3389/fmars.2018.00059>
- 1452 Stratmann T, Simon-Lledó E, Morganti TM, et al (2022) Habitat types and megabenthos  
1453 composition from three sponge-dominated high-Arctic seamounts. *Sci Rep* 12:.  
1454 <https://doi.org/10.1038/s41598-022-25240-z>
- 1455 Stratmann T, Voorsmit I, Gebruk A V., et al (2018b) Recovery of Holothuroidea population  
1456 density, community composition and respiration activity after a deep-sea disturbance  
1457 experiment. *Limnol Oceanogr* 63:2140–2153. <https://doi.org/10.1002/lno.10929>
- 1458 Stubbs CD, Smith AD (1990) Essential fatty acids in membrane: Physical properties and  
1459 function. *Biochem Soc Trans* 18:779–781
- 1460 Svensson PA, Wong BBM (2011) Carotenoid-based signals in behavioural ecology: A review.  
1461 *Behaviour* 148:131–189. <https://doi.org/10.1163/000579510X548673>
- 1462 Sweetman AK, Thurber AR, Smith CR, et al (2017) Major impacts of climate change on deep-  
1463 sea benthic ecosystems. *Elementa - Science of the Anthropocene* 5:.  
1464 <https://doi.org/10.1525/elementa.203>
- 1465 Tsushima M (2007) Carotenoids in sea urchins. In: Miller Lawrence J (ed) *Edible Sea Urchins:*  
1466 *Biology and Ecology*. Elsevier Science B.V., Amsterdam, pp 159–166
- 1467 Uhle ME, Macko SA, Spero HJ, et al (1997) Sources of carbon and nitrogen in modern  
1468 planktonic foraminifera: The role of algal symbionts as determined by bulk and compound  
1469 specific stable isotopic analyses. *Org Geochem* 27:103–113
- 1470 Uthicke S (1999) Sediment bioturbation and impact of feeding activity of *Holothuria*  
1471 (*Halodeima*) *atra* and *Stichopus chloronotus*, two sediment feeding holothurians, at Lizard  
1472 Island, great barrier reef. *Bull Mar Sci* 64:129–141

- 1473 van Deenen LLM (1966) Phospholipids and biomembranes. *Prog Chem Fats Other Lipids* 8:1–  
1474 127. [https://doi.org/10.1016/0079-6832\(66\)90003-6](https://doi.org/10.1016/0079-6832(66)90003-6)
- 1475 Veuger B, Middelburg JJ, Boschker HTS, Houtekamer M (2005) Analysis of <sup>15</sup>N incorporation  
1476 into D-alanine: A new method for tracing nitrogen uptake by bacteria. *Limnol Oceanogr*  
1477 *Methods* 3:230–240. <https://doi.org/10.4319/lom.2005.3.230>
- 1478 Volkman JK, Jeffrey SW, Nichols PD, et al (1989) Fatty acid and lipid composition of 10  
1479 species of microalgae used in mariculture. *J Exp Mar Biol Ecol* 128:219–240
- 1480 Vonnahme TR, Molari M, Janssen F, et al (2020) Effects of a deep-sea mining experiment on  
1481 seafloor microbial communities and functions after 26 years. *Sci Adv* 6:eaaz5922.  
1482 <https://doi.org/10.1126/sciadv.aaz5922>
- 1483 Wang J, Li J, Dasgupta S, et al (2014) Alterations in membrane phospholipid fatty acids of  
1484 gram-positive piezotolerant bacterium *sporosarcina* sp. DSK25 in response to growth  
1485 pressure. *Lipids* 49:347–356. <https://doi.org/10.1007/s11745-014-3878-7>
- 1486 Wiedicke MH, Weber ME (1996) Small-scale variability of seafloor features in the northern Peru  
1487 Basin: Results from acoustic survey methods. *Marine Geophysical Research* 18:507–526.  
1488 <https://doi.org/10.1007/BF00310067>
- 1489 Wigham BD (2002) The “Amperima Event”: Analysis of community change in the abyssal  
1490 Northeast Atlantic Ocean. PhD Thesis, University of Southampton
- 1491 Wigham BD, Hudson IR, Billett DSM, Wolff GA (2003a) Is long-term change in the abyssal  
1492 Northeast Atlantic driven by qualitative changes in export flux? Evidence from selective  
1493 feeding in deep-sea holothurians. *Prog Oceanogr* 59:409–441.  
1494 <https://doi.org/10.1016/j.pcean.2003.11.003>
- 1495 Wigham BD, Tyler PA, Billett DSM (2003b) Reproductive biology of the abyssal holothurian  
1496 *Amperima rosea*: An opportunistic response to variable flux of surface derived organic  
1497 matter? *Journal of the Marine Biological Association of the UK* 83:175–188.  
1498 <https://doi.org/10.1017/S0025315403006957h>
- 1499 Winemiller KO, Pianka ER (1990) Organization in natural assemblages of desert lizards and  
1500 tropical fishes. *Ecol Monogr* 60:27–55
- 1501 Witbaard R, Duineveld GCA, Kok A, et al (2001) The response of *Oneirophanta mutabilis*  
1502 (Holothuroidea) to the seasonal deposition of phytopigments at the Porcupine Abyssal Plain  
1503 in the Northeast Atlantic. *Prog Oceanogr* 50:423–441
- 1504 Wohlers J, Engel A, Zöllner E, et al (2009) Changes in biogenic carbon flow in response to sea  
1505 surface warming. *Proceedings of the National Academy of Sciences* 106:7067–7072.  
1506 <https://doi.org/10.1073/pnas.0812743106>
- 1507 Yano Y, Nakayama A, Yoshida K (1997) Distribution of polyunsaturated fatty acids in bacteria  
1508 present in intestines of deep-sea fish and shallow-sea poikilothermic animals. *Appl Environ*  
1509 *Microbiol* 63:2572–2577

1510 Yool A, Martin AP, Anderson TR, et al (2017) Big in the benthos: Future change of seafloor  
1511 community biomass in a global, body size-resolved model. *Glob Chang Biol* 23:3554–3566.  
1512 <https://doi.org/10.1111/gcb.13680>

1513 Zhao JX, Liu QQ, Zhou YX, et al (2015) *Alkalimarinus sediminis* gen. nov., sp. nov., isolated  
1514 from marine sediment. *Int J Syst Evol Microbiol* 65:3511–3516.  
1515 <https://doi.org/10.1099/ijsem.0.000446>

1516  
1517